Evaluation of upstream and downstream process parameters on Electrostatic Precipitator performance

GP Peens

20175116

Dissertation submitted in fulfilment of the requirements for the degree *Magister Engineering* in Mechanical Engineering at the Potchefstroom Campus of the North-West University

Supervisor: Prof CP Storm

May 2014

ABSTRACT

New emission legislation regarding air pollution control, as instructed by the Department of Environmental Affairs (DEA) to Eskom Generation Power Stations, implies a particulate emission limit of 100 mg/Nm^3 for all existing power stations by 2015 and 50 mg/Nm^3 for all new and existing power stations by the year 2020. Some of Eskom's power stations which are equipped with Electrostatic Precipitators (ESP's) were not designed for this stringent legislation. It is also experienced that ESP's and coal quality in Eskom have deteriorated over time, resulting in the performance of the ESP's not meeting the legislative requirements.

Eskom is in the process of introducing various ESP enhancement projects to improve performance and aligning the operating philosophy to comply with the more stringent particulate emission legislation.

An ESP efficiency test was conducted at Lethabo Power Station to determine the current state of the plant and performance. The results of the test were compared with the original design base specifications to determine the relevant deficiencies which contribute to high emissions and poor ESP performance.

It was aimed to develop an ESP simulation model and validate the outputs with the test data. This study endeavours to demonstrate the greater impact on ESP performance when the ESP is operated outside the design specification.

It is further aimed to demonstrate that a solution to the problem of high emissions is not only contributed by the variables within the ESP itself. This study is a coal to stack evaluation considering the ESP variables and the upstream conditions of the ESP that form part of the entire process. The intention of this study is to demonstrate the importance of operating an ESP at the designed parameters and highlight the significance of proper maintenance.

It was learned that before any ESP enhancement technology can be implemented, the ESP and upstream conditions must be in accordance with design specifications. The implementation of an ESP enhancement technology will have no merit or justification on a unit that is being operated outside of its design specifications.

The results obtained from the ESP simulation model correlated well with the ESP efficiency test data. The expectation of the model to assist operators and engineers to operate ESP's according to the designer's specifications was conceded.

KEYWORDS

Air heater leakage
Ash fineness distribution
Coal quality
Deutsch equation
Dust burden
Efficiency
Electrostatic precipitator
Matts-Ohnfeldt equation
Migration velocity
Optimisation
Particulate emission prediction
Performance
Power supply
Simulation model
Volume flow distribution

DECLARATION

I Gert Petrus Peens (Identity Number: 8503075195086) hereby declare that the work contained in this dissertation is my own work. Some of the information contained in this dissertation has been gained from various journal articles; text books etc, and has been referenced accordingly.

_____ _____

Initial & Name Witness

_____

ACKNOWLEDGEMENTS

I would like to thank Eskom and EPPEI (Eskom Power Plant Engineering Institute) for the support and opportunity to complete my M.eng (mechanical) at North West University. I am thankful for the opportunity to utilise test data obtained from Eskom's database to complete this study.

I also would like to express the deepest appreciation to Professor Chris Storm, who undertook to act as my supervisor. Without his guidance and persistent help this dissertation would not have been possible

DEDICATION

To the three remarkable women in my life: my grandmother, my mother and my wife

CONTENTS

LIST OF TABLES

LIST OF FIGURES

NOMENCLATURE

CE	Collecting Electrode
CFD	Computational Fluid Dynamics
DE	Discharge Electrode
DEA	Department of Environmental Affairs
EDF	Electricity de France
EES	Engineering Equation Solver
EPRI	Electric Power Research institute
ESP	Electrostatic Precipitator
FD	Forced Draft
FFP	Fabric Filter Plant
FGC	Flue Gas Cleaning
GO	General Overhaul
HF	High Frequency
HV	High Voltage
Hz	Hertz
ID	Induced Draft
IRS	Ingegneria Ricerca Sistemi
kHz	kilo Hertz
kV	kilo Volts
LHI	Left Hand Inner
LHO	Left Hand Outer
mA	milli Ampere
MCR	Maximum continues rating
mg/Am^3	Milligram per actual cubic meter
mg/Nm^3	Milligram per normall cubic meter
mg/Sm^3	Milligram per standard cubic meter
MW	Mega Watt
MWe	Mega Watt electric
OCGT	Open Cycle Gas Turbines
PA	Primary Air
PCLF	Planned Capacity Loss Factors
PF	Pulverised Fuel
PFFR	Pulverised Fuel Firing Regulation

ppm	Parts per million
RHI	Right Hand Inner
RHO	Right Hand Outer
SCA	Specific Collecting Area
SoRI	Southern Research Institute
TR	Transformer Rectifier
U	Unit
P_{STAG}	Stagnation Pressure
P_{STAT}	Static Pressure
P_{DYN}	Dynamic Pressure
HX_{EFF}	Heat Exchanger Effectiveness

1 INTRODUCTION

1.1 BACKGROUND

Eskom, the only power generation utility in South Africa has a combined power generation capacity of 44318 MWe. This capacity is a combination of Coal Fired P, Nuclear, Hydroelectric, Pumped Storage, and Gas Turbine Power Stations. The 44318 MWe generated by Eskom is divided as follows:

Table 1.1: Coal-Fired Power Stations in Eskom

Arnot	2400 MW
Duvha	3600 MW
Hendrina	2000 MW
Kendal	4116 MW
Kriel	3000 MW
Lethabo	3708 MW
Majuba	4110 MW
Matimba	3990 MW
Matla	3600 MW
Tutuka	3654 MW
Camden	1600 MW
Grootvlei	1200 MW
Komati	1000 MW

Table 1.2: Nuclear Power Stations in Eskom

Koeberg	1931 MW

Table 1.3: Hydroelectric and Pumped Storage

Drakensberg Pumped Storage Scheme	1000 MW
Palmiet Pumped Storage Scheme	400 MW
Gariep	360 MW
Vanderkloof	240 MW

Table 1. 4: Gas Turbines (Open Cycle Gas Turbine)

Acacia	171 MW
Port Rex	171 MW
Ankerlig	1327 MW
Gourikwa	740 MW

Table 1. 5: New build power stations in Eskom

Medupi, Coal Fired	4800 MW
Ingula, Pumped Storage Scheme	1332 MW
Kusile, Coal Fired	4800MW
Tubatse, Pumped Storage Scheme	1500MW
Sere Wind Farm	100MW
Wind 500	500MW

Eskom makes use of two Flue Gas Cleaning (FGC) technologies namely Electrostatic Precipitators (ESP's) and Fabric Filter Plants (FFP's). Half of the total capacity (21647 MWe) is generated with coal fired power stations equipped with electrostatic precipitators.

Table 1. 6: Flue gas cleaning technologies in Eskom

Power Stations equipped with FFP's (Fabric Filter Plants)		
- Arnot	FFP	
- Camden	FFP	
- Duvha (partially)	FFP	
- Grootvlei (partially)	FFP	
- Hendrina	FFP	
- Majuba	FFP	
Percentage of Eskom's fleet fitted with FFP's		**43%**
Power Stations fitted with ESP's (Electrostatic Precipitators)		
- Duvha (partially)	ESP	
- Grootvlei (partially)	ESP	
- Kendal	ESP	
- Kriel	ESP	
- Matla	ESP	
- Tutuka	ESP	
- Lethabo	ESP	
- Matimba	ESP	
Percentage of Eskom's fleet fitted with ESP's		**57%**

ESP's have been used for the past 90 years to collect particular matter in industrial flue gases before the gas is emitted into the atmosphere. According to (Porle, Francis, & Bradburn, 2005) the first ESP's for the collection of fly ash exiting coal fired furnaces were constructed in 1920. An ESP or electrostatic gas cleaner is a

particulate collection device that removes particles from a gas stream using the force of an induced electrostatic charge. Coal fired power stations, cement industries, paper industries and foundries are industries that regularly make use of ESP's. The flue gas generated by the combustion process in a furnace is evacuated through a gas duct to the ESP inlet. The performance (efficiency) of an ESP is dependent on a number of parameters, some of which are directly related to the ESP (dependant parameters) and others that are indirectly (independent parameters) related to the ESP. The ESP comprises of a set of parallel casings to encapsulate the particular matter in the gas stream. The internals of an ESP is comprised of a series of repeating electrodes, one connected to a high voltage source (discharge electrodes) and the other grounded (collecting electrode). With high voltage applied to the discharge electrodes an electrical field is generated between the electrodes. As the flue gas passes through these electrical fields the gas particles are ionised with negative ions migration towards the grounded electrode. During the migration of the negative ions towards the collector electrode, the ions collide with and attach themselves to the solid particles (known as particle charging) in the gas stream and are drawn towards the collector electrodes.

A layer of ash particles accumulate on the collecting electrodes until the ash is dislodged to clean the electrodes to provide space for new particles to be collected. The collecting electrodes are periodically rapped (by means of a hammer striking an anvil connected to the collecting electrode) dislodging the accumulated ash to the discharge hoppers. The continuous process of charging the particles, collecting the particles and dislodging the particles are the three steps in which an ESP process functions. Figure 1.1 indicates the gas flow direction, the ionisation of the ash particles and the accumulation of the ash particles on the collector electrodes

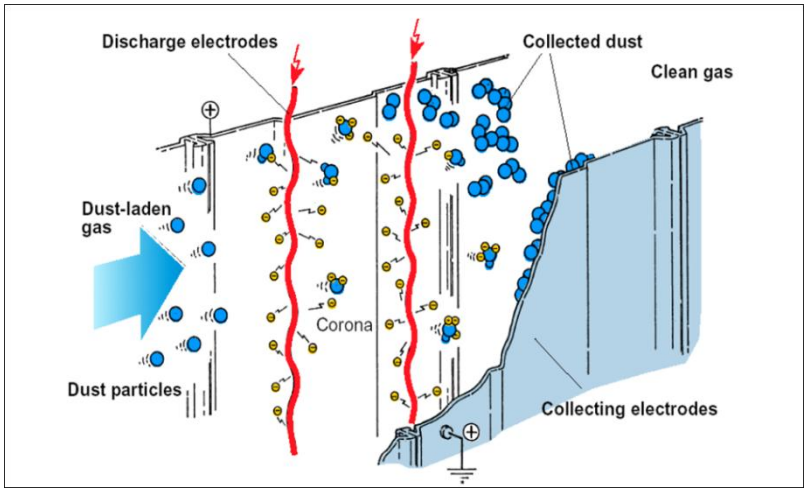

Figure 1.1: ESP operating philosophy (Porle, Francis, & Bradburn, 2005)

Eskom is constantly challenged to operate coal fired power stations within the particulate emission limits set by the Department of Environmental Affairs (DEA). Each power station in Eskom has an emission limit to comply with, based on the Flue Gas Cleaning technology and operation conditions. The FGC plant is situated at the back end of the furnace (furnace outlet) to collect the particular matter (ash) produced by the combustion process. In the event of a power station exceeding the specified emission limit, the power station can be forced to shut the unit down or to reduce the operating load (reduced load results in less coal being burned therefore less ash is produced that has to be captured by the Flue Gas Cleaning plan). The consequence of operating at a reduced load is, firstly, that the power generation capacity is reduced, resulting in less electricity being available to the electrical network. Secondly, in high electricity demand periods, operating at reduced loads can lead to load shedding negatively impacting on the South African economy. The main contributing factor to Eskom power stations operating above the emission limit is either the underperforming of the FGC plant or the underperforming of the ash handling plant. The ash handling plant is responsible for removing the ash collected by the ESP from the ESP hoppers. From there the ash is conveyed to the ash disposal for storage.

New emission legislation with regards to air pollution control, instructed by the Department of Environmental Affairs (DEA) to Eskom Generation Power Stations (Air Quality Act, 2004 [Act 39/2004], Notice 248; 31 March 2010: Minimum Emission Standards) implies the following:

- **Particulate matter:**
- Less than 100 mg/Nm^3 for all existing power stations by 2015
- Less than 50 mg/Nm^3 for all new power stations by 2020

- **Sulphur dioxide:**
- Less than 3 500 mg/Nm^3 for all existing power stations
- Less than 400 mg/Nm^3 for all new power stations

- **Oxides of nitrogen:**
- Less than 1 100 mg/Nm^3 for all existing power stations
- Less than 650 mg/Nm^3 for all new power stations
- All plants to have continuous emissions monitoring for particular matter, SO_2, NO_x by end of 2013.
- Mercury (not part of minimum emissions standards):
- All concentrations are normalised to the following: standard temperature and pressure at 10% O_2 on a dry basis (maximum hourly releases).

There are mainly 6 causes for Eskom's power stations not meeting the specified station emission limit:

1. The design specifications of older plants were specified to comply with the emission legislation during the time of design and construction.
2. Deterioration of plant and equipment.
3. Coal quality deterioration.
4. More stringent emission legislation.
5. Scheduled outages are postponed due to a constrained electrical network supply; therefore important maintenance is reduced.
6. Expertise of workmanship and quality control during outages.

For an Eskom employee employed in the air quality control department, these are the 6 challenges that are dealt with on a continual basis.

The data depicted in Figure 1.2 stress the need for Eskom to develop an emission control strategy to lower particulate emissions that will put Eskom in the position to operate below the emission limits. The figure indicates that Eskom did not meet its targets for 8 of the 12 months for the financial year of 2011/2012. It is evident that there is a need to lower the particulate emissions to the desired target levels.

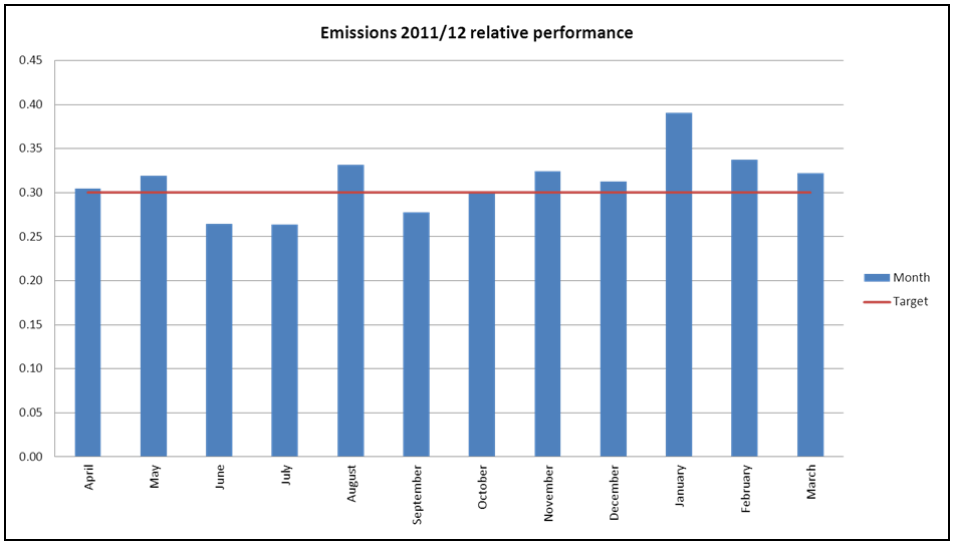

Figure 1. 2:Eskom 2011/2012 relative emissions performance against target.

1.2 PROBLEM STATEMENT

- Eskom experiences a problem with incipient non-complying particulate emissions, worsened by more stringent legislation for the immediate future.
- The implementation of existing ESP enhancement technologies is needed.
- Replacing ESP plant and retrofitting with FFP is the current plan of action envisaged, but with certain constraints:
  - FFP retrofit is very expensive (R600 billion per station).

  - Also, FFP are sensitive to high back-end temperatures, where the current operating regime often exceeds the 180 ^{0}C limit of flue gas temperature.
  - Bag filters require extended outage durations of up to 120 days, which is not favourable for the increasing electricity demand.
  - Some Power Stations are approaching the end of their life-expectancy, thus it is deemed more beneficial to enhance the performance of the existing assets.
- ESP modelling software programs do exist, with the following constraints:
  - It is generic programs more intended for design.
  - Due to the protected code and associated intellectual property, the user is limited to the user interface and oblivious to exactly what the criteria leading to the answers were.
  - The limits and boundaries vary between the different software packages and the focus areas and objectives differ between models.
- A simulation model is thus needed to serve as a diagnostic tool to evaluate a unit from “coal-to-stack” and forecast particulate emissions emanating from out-of specification process parameters, utilising the existing ESP plant to the optimum.

1.3 OBJECTIVE

- To develop a simulation model that incorporates all the dependant and independent parameters to evaluate the performance of the ESP
- The simulation model is then to be validated with ESP efficiency test data from Lethabo Power Station
- To demonstrate the greater impact on ESP performance when the ESP is operated not according to design specifications
- To categorise the various parameters by identifying which parameters contribute most to poor ESP performance.
- To demonstrate that a solution to the problem of high emissions is not only contributed by the dependant variables within the ESP itself.
- To compile a simulation model that will predict ESP performance with adequate accuracy within realistic operating scenarios.
- Identify which ESP enhancement technologies will be suitable for Eskom Power Stations equipped with ESP’s

1.4 RESEARCH METHODOLOGY

- Identify the functions that the model has to fulfil, i.e. the upstream and downstream process parameters that will impact on final stack emissions.

- Perform a literature survey on the technical criteria of ESP functioning, identifying all the process parameters and the formulae governing ESP performance.
- Also, perform a literature survey of existing technology to ascertain the availability and usability of ESP simulation models.
- Categorise the dependant and independent variables impacting on ESP operation
- In this case, where the need for a more customised simulation model is to be developed, a suitable code is to be investigated.
- Perform the programing of the model logic.
- Obtain data from tests performed on the ESP concert to verify the results produced by the simulation model.
- Use the simulation model to predict ESP performance due to out-of-specification process parameters.
- Categorise the degree of impact by out-of-specification process parameters on ESP performance within realistic limits of variance.

1.5 SCOPE AND LIMITS OF THE STUDY

- The simulation model is developed for Lethabo Power Station ESP's
- Intensive evaluation of certain elements in the process will not be covered in the study such as: mill, burner and air heater performance, but only the result of out of specification functioning, such as leakage, high air and gas flow, etc.
- Dependant parameters namely: Re-entrainment, rapping losses, waveforms of the power supply and the injection of SO_3 will be excluded from this study.
- For the development of this ESP simulation model it is assumed that the velocity profile and gas flow distribution will remain constant throughout the ESP.

1.6 DISSERTATION STRUCTURE

Chapter 1

Chapter 1 provides information regarding the initiation of the study and facts that lead to the study. This entails the identification of the deficiency. Various solutions to the problem are evaluated and briefly discussed. The dependent and independent ESP parameters that have an influence on the ESP performance are defined. The problem to be investigated is stated as well as the goals, limits and objectives of the study.

Chapter 2

Chapter two discusses the survey that was carried out on the topic to ensure that all the relevant aspects affecting ESP performance were identified. These aspects are required to develop an ESP simulation model.

Chapter 3

Chapter 3 provide information on ESP enhancement technologies. The upstream and downstream parameters affecting the efficiency of the of the ESP are stipulated in this chapter

Chapter 4

Chapter 4 expounds the method of the data gathering as well as the test program and test requirements. Test execution, test preparation and test results are also discussed.

Chapter 5

The chapter describes some of the important equations used and how these equations are derived. Explanations are provided on why specific equations and formulas are used above others. It covers the requirements and how the findings and results were obtained.

Chapter 6

Chapter 6 includes an interpretation of the results obtained from the ESP simulation model and how the model correlates to the test results. Recommendations to improve the ESP simulation model are discussed along with recommendations for future studies.

Chapter 7

In chapter 7 the references are listed according to the NWU Harvard method.

Chapter 8

Chapter 8 includes appendix A and appendix B

---

2 LITERATURE SURVEY AND EXISTING TECHNOLOGIES

Engineers often make use of mathematical or computer models to design ESP's. These models can be used to predict the particulate emissions and the efficiency of the ESP. These models are also used to predict the expected ESP performance when considering an ESP enhancement technology. Most of these models are based on the Matts-Ohnfeldt equation (K.R, 1997) to determine the efficiency.

The Southern Research Institute (SoRI) developed one of the first mathematical models 1975 (Faulkner & DuBard, 1984), which relates the collection efficiency to the ESP size and various operating parameters. Over the years the model has been improved to accommodate a wider range of criteria and scenarios, increasing the reliability of the model. The problem experienced with a lot of these models is that users are limited to the user interface. If the model provides the user with an answer, the user is oblivious of how the answer was obtained and what the criteria influencing the results were. This is understandable due to the intellectual property and code protected by the program developer. Some models only take curtain parameters into account and the limits and boundaries vary substantially between the different models available. The reason for this is that various models are designed with different focus areas and objectives. Some models focus intensively on the migration of a dust particle from the discharge electrode to the collecting electrode, where other models have a more holistic focus. Table 2.1 lists the input data used in the SoRI model, this data is used to calculate the required parameters.

Table 2.1: Input data for ESP simulation models (Harris, 2003)

ESP Specifications	Gas/particulate specifications
Estimated efficiency	Gas flow rate
Precipitator length	Gas pressure
Superficial gas velocity	Gas temperature
Fraction of sneakage / re-entrainment	Gas viscosity
Normalized standard deviation of gas velocity distribution	Particulate concentration
Number of stages for sneakage / re-entrainment	Particulate resistivity
Number of electrical sections in direction of gas flow	Particulate density
For each electrical section	Particle size distribution
Length	Dielectric constant
Area	Ion speed
Applied voltage	
Current	
Corona wire radius	
Corona wire length	
Wire-to-wire spacing	
Wire-to-plate spacing	
Number of wires per linear section	

Orchidee is an ESP simulation model developed by Electricity de France (EDF) and Ingegneria Ricerca Sistemi (IRS). Orchidee is a tool that takes most of the dependent and independent parameters into account to predict the ESP performance. Orchidee is a simulation tool developed for optimization of the ESP's. It evaluates the efficiency of the electrostatic precipitators, once the operating conditions of the plant are provided. The evaluation is based on physical models of the combustion conditions and of the electrostatic precipitation processes.

To develop an ESP simulation model it is important to classify all the parameters that contribute to the performance of an ESP. It is important to know the significance of changes in the various parameters on ESP performance. This chapter discusses the entire process as the coal and ash particles voyage through the furnace and highlights all the parameters that have an influence on ESP performance.

The different plant areas of a power station are sometimes operated as if they're isolated from one another, while in reality every piece of equipment in the system has an influence on the downstream equipment. It is very important to note that

finding a solution to the problem of high emissions must not be a symptomatic approach by optimising and enhancing only the dependant variables within the ESP itself. It is a root cause approach by evaluating the upstream independent variables along with dependent variables.

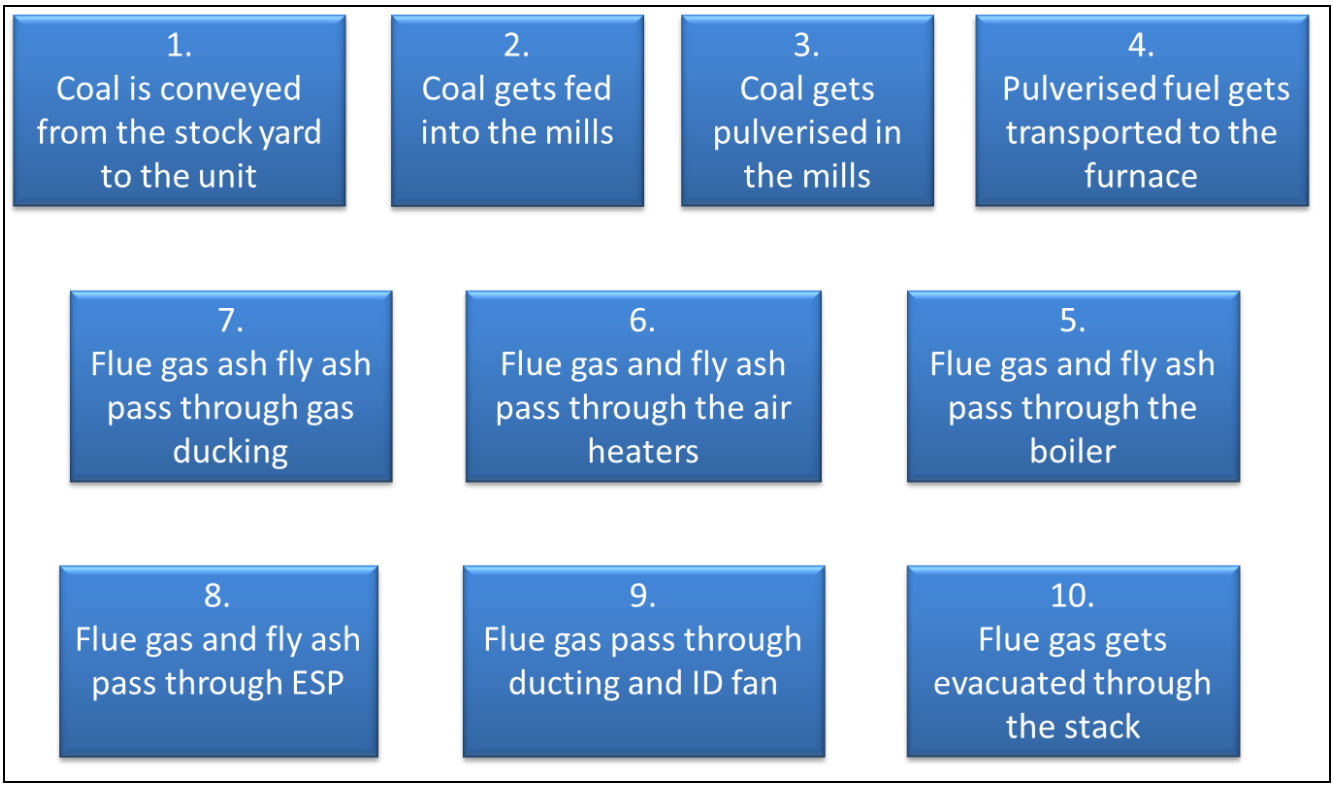

Figure 2.1: Migration of coal through a furnace

Figure 2.1 illustrates 10 steps on the coal to ash process. Each block in the figure represents a plant area or a property of a component. Consider block number 1 - Coal: What is the effect on ESP performance with variation in coal quality, and what properties of coal have the most significant influence on ESP performance?

The literature is focused to determine the effect and impact on ESP performance when the entire process (block 1 to 10) is considered. The methodology consists of determining what the influence and significance of each block has on the ESP performance. It is then important to incorporate all relevant aspects into the ESP simulation model.

2.1 COAL QUALITY:

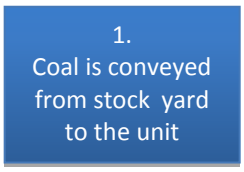

Coal is the very first product that forms part of the process to generate electricity. The combustion of coal produces ash; the ash is then encapsulated by the ESP. It is therefore be deduced that the quality and properties of the coal determines the properties of the ash. There are various aspects of coal quality that influences the ESP efficiency. According to (Srinicasachar, Johnson, Senior, & Durham) coal quality effects ESP efficiency in several ways, namely:

- Sulphur content in the coal,
- Ash content of the coal,
- Chemical composition of the fly ash affects the ash resistivity,
- Fly ash size distribution is determined by the type of coal and the coal mineralogy and combustion process.

One of the biggest contributors to ESP performance is the percentage of ash in the coal and the ash resistivity. The initial ash percentage in the coal cannot be converted into energy, therefore the ash that enters the furnace must exit the system by means of the flue gas cleaning technology and the stack. When an ESP is designed and sized, ash percentage and ash resistivity is one of the first parameters to take into account.

Coal analysis has two different types of references namely proximate and ultimate analyses.

Proximate analysis is classified as:

Table 2. 2: Proximate analysis

$Carbon_{Fixed}$(by difference)
Volatile matter
Ash
Surface moisture
Inherent moisture
Total moisture
Gross calorific value

Ultimate analysis is classified as:

Table 2. 3 : Ultimate analysis

Nitrogen
Oxygen (by difference)
Carbon $_{Total}$
Ash
Sulphur
Hydrogen
Surface Moisture
Inherent Moisture
Total moisture

The percentages of all of these properties have an influence on the combustion process. The combustion process then determines the product that will be evacuated to the ESP. The impact on ESP performance with variation of the coal quality will have different effects from plant to plant, due to different designs. Another property of coal having an effect on ESP efficiency is the Hardgrove index of the coal. This is an empirical number, which relates to the ease with which coal can be ground. The Abrasiveness Index of coal is an indication of the abrasiveness of coal expressed as mg Fe/kg loss. Both these properties of coal have an influence on the coal fineness, particle shape and size.

From the above it can be concluded that the first product (coal) required for power generation has a significant influence on the downstream parameters which will affect the ESP performance.

2.2 COAL FEED RATE:

Coal is stored in massive coal bunkers above the coal feeders. The coal feed rate is mainly determined by furnace load. The feed rates of the feeders are governed by variable speed drive motors. The higher the furnace load the higher the coal feed rate. For Lethabo Power Station the coal feed rate at 600 MW is 100 kg/s. If for argument's sake the ash percentage of the coal is 35% then the ESP must handle 35 kilogram of ash per second. Coal quality also has an influence in the coal feed rate. One will require a higher coal feed rate for poor coal quality than for a good quality coal for the same energy output.

2.3 COAL FINENESS:

The next process in line is the milling plant. The mills are the first components of the furnace that affects the performance of an ESP. Depending on the type of mill (vertical spindle mill or tube mill), the settings determine the fineness of the PF conveyed to the burners. The mills determine the basic particle size distribution of the ash entering the ESP. When considering a tube mill, the mill load (ton of grinding balls in the mill) determines the coal fineness. Chapter 2.16 looks in more detail at the effect of particle shape and size on ESP performance. The smaller a segment of coal is grinded, the larger the surface area exposed to the flame temperature in the burner. Smaller particles can therefore release more volatilise, encouraging combustion and releasing more heat. The fineness of the coal also has an influence on the furnace back-end temperatures. The burnout time determines the height of the heat release barrier. Larger particles have a longer residence time, therefore the heat release barrier will shift higher up in the furnace increasing the back-end temperatures. The effect of high ESP inlet temperatures on ESP performance is discussed in chapter 2.9

Furnace manufacturers normally specify a coal grind based on a sieve test which breaks the sample of coal leaving the mill into four segments of size. The most common standard for these sizes of the sieves are standardized as a 50-mesh, 100-mesh, and 200-mesh screen corresponding to 290-micron openings for the 50-mesh and 74-micron openings for the 200-mesh screen. The micron is a minute measurement and represents one thousandth of a millimetre. For practical purposes the amount of coal larger than 290 microns and passing the 74-micron sieve are of most interest. It is this kind of coal, as well as 290-micron segment coal that causes the furnace and ESP to operate under undesirable conditions. Coal fineness of over 0.5% retained on 50 mesh (99.5% through) or less than 80% through 200 mesh can cause increased carbon carry-over to the ESP. Some mill difficulties could jump this large size segment into the 2% to 4% by weight range, which would generally result in a large part of these outsized coal particles leaving the combustion zone in an unburned state (Harris, 2003). From the above it can be deduced that there is an optimum coal fineness for each furnace to accommodate the combustion requirements and the ESP requirements.

2.4 TOTAL AIR SUPPLIED TO FURNACE:

4.
Coal gets transported
to the furnace

For combustion of coal, three important products are required namely: coal, temperature and oxygen in the correct ratios. The correct mixture of coal and air will provide optimum combustion. According to (Storm, 1998) substantial overall efficiency can be gained with optimum air flow The total air supplied to a furnace is supplied by the primary air (PA) and Forced Draft (FD) fans. The quantity of air supplied is mainly controlled by the furnace load and coal quality. The O_2 measurement at the economiser outlet provides an indication of the amount of air supplied to furnace and can be adjusted accordingly. Figure 2. 2 illustrates the total air supplied to the furnace.

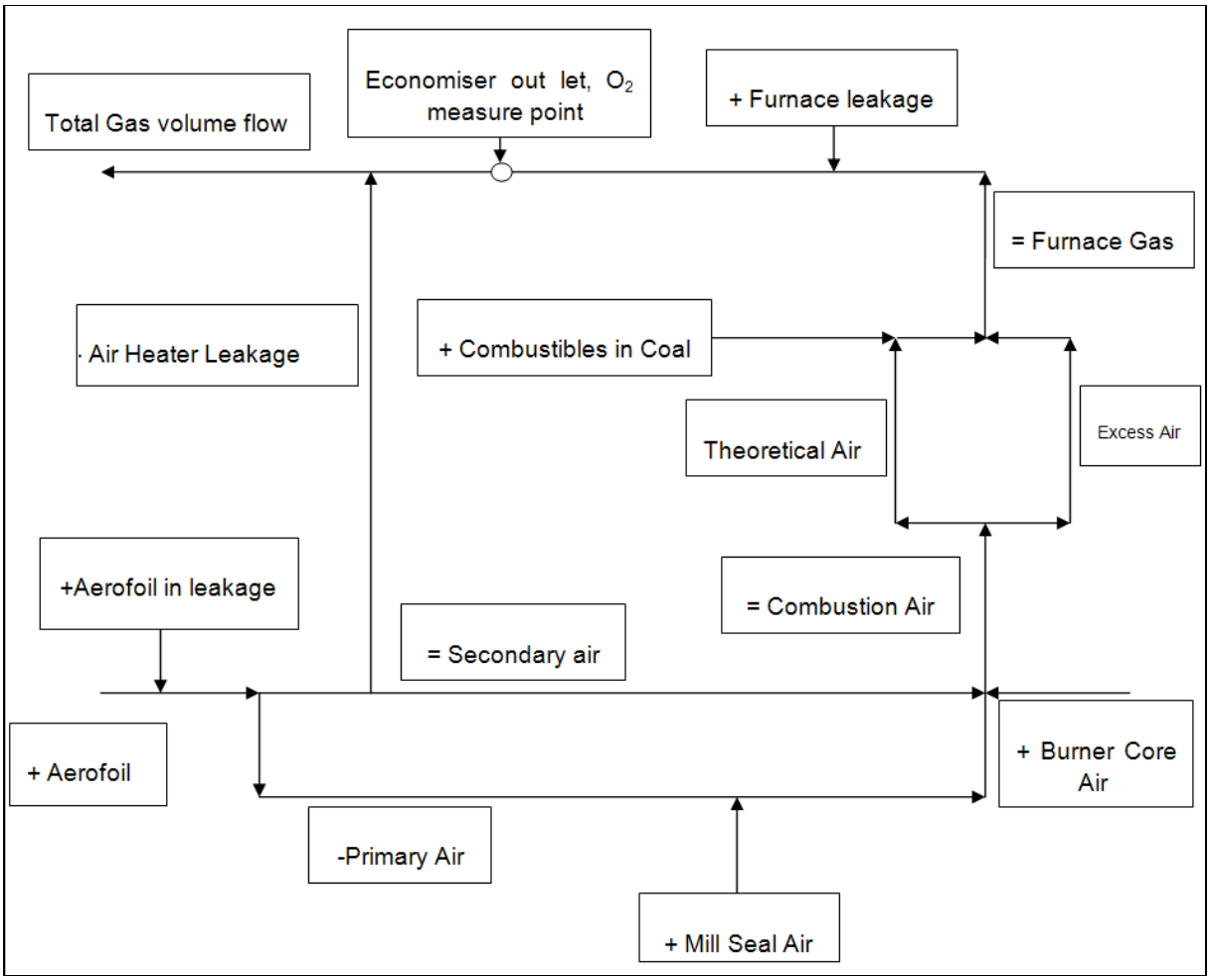

Figure 2. 2 : Air and flue gas flow diagram (Storm, 1998)

2.5 EXCESS AIR

The O_2 reading measurement at the economiser outlet is a very important measurement for furnace and ESP operators. This single measurement combines the gas flow rate, gas temperature, and combustion information into one mix of factors that affect the ESP. The O_2 reading primarily represents the amount of excess air needed in the furnace combustion process. Most utility furnaces will be seen to operate in the 1.5 to 4% range of O_2. The most common number will hover around the 3% average level of O_2 at the economiser outlet.

One of the main reasons for operating at a higher average O_2 is to play it safe in a complex combustion environment. For this reason, most furnaces run at 16% to 20% average excess air at full load, as determined by the O_2 measurement that is carefully observed in the control room of the unit. Although the O_2 reading may not always represent a true average of O_2 at all times, it still provides a useful monitor of the changes in the flue gas. (K.R, 1997)

2.6 TOTAL FLUE GAS VOLUME FLOW

When considering the Deutsch equation it will be noted that volume flow is a function of the Deutsch equation (Porle, Francis, & Bradburn, 2005). The volume flow determines the velocity and particle treatment time through the ESP. The volume flow through the ESP is determined by the total air supplied to the furnace, excess air, furnace in leakage and air heater leakages. All these parameters equate to a total volume flow presented to the ESP. The furnace in leakages and air heater leakages equates to a higher total volume flow that the ESP will have to handle. Keeping in mind that the ESP may not be designed for these operating conditions and high volume flows. Therefore under such condition the ESP efficiency will not be according to the design base and poor ESP performance can be expected. It is therefore important to identify the effects and significance of high volume flow related to ESP efficiency.

2.7 TOTAL FLUE GAS MASS FLOW

An ESP will be designed to handle a specific mass flow or dust burden. The mass flow is determined by the percentage ash in the coal and the coal feed rate. In the South African context export coal with an ash percentage of between 12% and 18% will have a lower ash burden. Power stations burning these types of coal will be designed with smaller ESP's. Lethabo Power Station burns a unique coal with an ash percentage that ranges between 35% and 41%. Therefore Lethabo Power Stations have some of the biggest ESP's in the world due to the unusually large ash burden.

The bottom ash to fly ash ratio affects the mass flow that will be conveyed through the ESP. The bottom ash is coarse and porous and is collected in the hoppers beneath the furnace. These bigger and heavier particles are not entrained by the

gas stream and fall down to the furnace hoppers (K.R, 1997). According to the Lethabo Power Station specification the bottom to fly ash ratio is 96.3% fly ash and 3.7% bottom ash.

In the process of developing an ESP simulation model it is important to factor for the correct mass flow and accommodate for the bottom to fly ash ratio.

2.8 AIR HEATER PERFORMANCE

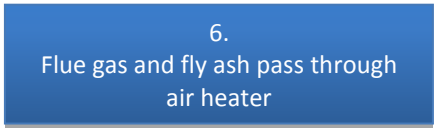

The air heater is usually the last piece of equipment of the furnace before the flue gas enters the ESP. For Lethabo Power Station there are four air heaters situated at the outlet of the furnace namely: Secondary and primary air heaters for the left hand side and secondary and primary air heaters for the right hand side. The air heaters transfer some heat from the hot flue to pre-heat combustion air. The heat exchange between the hot gas and cold air produces a significant reduction in the flue gas temperature, from ± 350°C to ±130°C. Therefore the air heater performance plays a major role in the total plant performance (Storm, 1998). An air heater in a poor condition can result in high ESP inlet temperatures and low combustion air temperatures. The effect on ESP performance with regards to high ESP inlet temperature is discussed in chapter 2.9

Air heater performance is not only measured by the rate of heat exchange but also by air heater leakage. Since the gas stream is under negative pressure and the air stream under positive pressure, excessive amounts of air can leak into the gas stream if the condition of the air heater is not in a good state. If the air heater leakage is above an expected level the consequences are poor heat exchange between the air and gas streams and the volume flow towards the ESP is increased. Figure 5. 4 explains this theory.

2.9 FLUE GAS TEMPERATURE

ESP gas inlet temperature plays a significant role when it comes to ESP efficiency. When considering all the variables in the Deutsch equation, two of the three variables, namely volume flow and migration velocity, are affected by temperature. It can be expected that change in ESP inlet temperature has an effect on the ESP performance.

There are many factors affecting the flue gas temperature.

From the furnace side:

- Particle size and particle burn-out time.
- Height of the heat release barrier.
- Condition of the furnace, dirty or clean furnace.
- Air heater performance.
- Soot blowing.
- Air ingress.

From the outside plant:

- The distance of the ductwork between the air heater to the ESP inlet,
- Air ingress on the ESP duct
- Length of the ESP
- Air in-leakage into the ESP
- Condition of the insulation for the ductwork and the ESP
- The effect of radiant cooling will alter the temperature profile in the ESP.

Changes in the furnace load with its resultant fan capacity will move temperatures up and down. Shifting the amount of air through each F.D. fan will change the gas temperatures exiting the air heaters. Even at the same production rate, minor changes in the excess air or staging of the mill loads can shift combustion zones, effecting exit flue gas temperatures. Some utilities are equipped with by-pass air ducts around the air pre-heaters and several methods for heating incoming air to the F.D. fans. The settings and condition of components related to the by-pass air and air heaters have an effect on the flue gas temperature (Harris, 2003). When considering volume flow, any gas expands when heated due to the intermolecular reactions. Since the volume of the ESP casing remains constant the volume flow through the ESP will increase, which will result in higher gas velocities through the ESP, discussed in chapter 2.11. The flue gas viscosity is also affected by the gas temperature. As the gas temperature increases, the gas viscosity increases. A higher gas viscosity reduces the particle migration velocity therefore affecting the collection efficiency of the ESP. The effect of gas viscosity is discussed in chapter 2.17.

It is important to always operate with ESP inlet temperatures that are above the acid dew point of the gas to avoid corrosion and reduce dust build up due to sticky ash. SO_2 and SO_3 are formed in the combustion of coal. These gases react with H_2O and form H_2SO_4 gas. The amount of SO_3 in the gas stream determines the acid dew point temperature. When H_2SO_4 gas condenses sulphuric acid is formed, which is a very aggressive acid and which can cause severe damage to the plant. Corroded components will reduce the reliability of the ESP and affect

the performance of the ESP. Another parameter that changes with variation in temperature is ash resistivity, which is discussed in chapter 2.19.

In conclusion, flue gas temperature affects the gas volume, gas viscosity and ash resistivity. From the above it could be seen that flue gas temperature has significant effects on the performance of an ESP. When calculating ESP efficiency it is important to identify the effect of temperature on volume flow and distinguish between the parameters that change.

2.10 VOLUME AND MASS FLOW DISTRIBUTION BETWEEN CASINGS

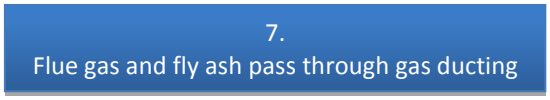

The volume flow distribution between the ESP casings must not be ignored. Often industries do not realise the impact of volume flow distribution between the 4 casings. Mal-distribution between casings can produce a situation where one casing can be overloaded compared to others. Figure 2. 3 indicates a scenario where the left hand outer casing is totally overloaded compared to the right hand outer casings. The left hand inner casing sees a higher volume flow that increases the velocity as well as a higher dust loading. It can be expected that this casing is not designed for this condition and therefore will not perform well. According to (Mudry, 2002) the flow within each chamber must be within ±10% of its theoretical share. If the theoretical share is 25%, then the flow cannot be less than 22.5% or higher than 27.5%.

Mal-distribution between casings is mainly produced by an off-balance draft group. Induced draft (ID) fan amps (block nine), forced draft (FD) fan amps and damper setting can be used as an indication of mal-distribution between casings. Air leakage at the seals of the air heater can produce a significant amount of air leaking from the FD fan system (positive pressure) to the flue gas side (negative pressure) controlled by the ID fan. Even with new seals, air leakage across the air pre-heater could reach 7% to 9% levels. The percentage leakage between the left hand and right hand air heaters can vary significantly enforcing mal-distribution between the 4 casings (Mudry, 2002).

Another reason for mal-distribution is caused by turning vanes located in the gas ducting. Turing vanes are exposed to excessive erosion caused by the fly ash. Fly ash travelling at speeds of 12-18 m/s can severely erode steel columns,

distribution screens, struts and turning vanes in a matter of months. Poor maintenance on the turning of the vanes can cause the flow to be more biased towards one casing compared to another.

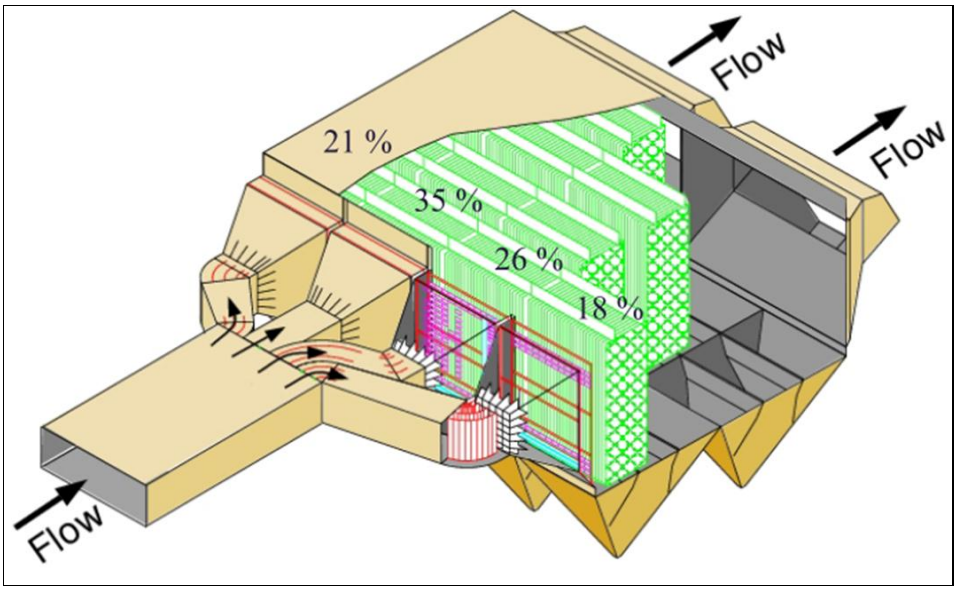

Figure 2. 3 : Volume flow distribution between ESP casings

2.11 FLUE GAS VELOCITY

8.
Flue gas and fly ash pass through the ESP

The gas flow velocity is primarily determined by the draft generated by the ID fan. The volume flow is a function of the cross section area and the velocity. The velocity in the ESP ranges between 0.8 and 1.2 m/s. Over the years a number of ESP efficiency tests have proven that the migration velocity is affected by gas velocity, reducing the ESP efficiency (K.R, 1997). High gas velocities reduce the particle treatment time. This is the time required for the particle to travel from the ESP inlet to the ESP outlet. Therefore less time is available to charge and collect ash particles. Another concern with high gas velocities is re-entrainment and sneakage. In the scenario where high gas temperatures and high gas velocities are experienced,.the adhesion and cohesion forces acting on the particles are also reduced by high gas temperatures. The forces acting on the particles in the dust layer are not strong enough to keep the ash layer together in high velocity areas and the ash particles are re-entrained into the gas stream (McCain, 2007)

High gas velocities can re-entrain ash in the hoppers (already collected particles) back into the gas stream if the hoppers are overfilled and if the hopper baffles are not in a good state. Figure 3. 3 illustrates the position of the hopper baffles to

reduce re-entrainment. High gas velocities encourage re-entrainment during rapping, which is known as rapping losses as discussed in chapter 2.13. For optimum ESP operation it is important to always operate the ESP with design base gas velocities to eliminate poor collection efficiency and reduce re-entrainment.

2.12 RAPPING

For an ESP to operate at optimum efficiency, it is necessary to clean the discharge and collector electrodes. The polarity of the particles depends on which electrode the particles will deposit. A particle will always deposit on the electrode with an opposite polarity. The accumulated ash on the electrodes has to be dislodged to make place for newly charged particles to be collected.

The discharge and collector electrodes are periodically rapped to clean the electrodes so that the ash build-up on the electrodes has a minimum effect on the electrical operating conditions. The duration (how long) and interval (how frequent) of the rapping are determined by the rate of deposition. Therefore the rapping philosophy will vary from the inlet field to the outlet field, since the deposit rate varies from the inlet to the outlet field. It is important to enable the deposited layer to achieve a sufficient thickness of 1000µm when sheared from the surface of the electrode. Thus there is an optimum thickness of the dust layer at which the electrode must be rapped (Popvici, 1996).

There are various rapping techniques that can be implemented to find an optimum rapping philosophy. Eskom makes use of the following rapping techniques:

- Reduced power rapping
- Full power rapping
- Off power rapping
- Master rapping
- Clean rapping
- Rapper queuing
- Test rapping

It is very difficult to theoretically determine the optimum rapping philosophy for an EPS. Theoretical indications can be used as a baseline but fine-tuning and optimisation takes days of experimenting with various intervals and durations. It is years of experience rather that will enable an ESP engineer to master the rapping philosophy. It is experienced that with an optimised rapping philosophy particulate emissions can be reduced by 30%.

2.13 RE-ENTRAINMENT AND RAPPING LOSSES

The concept ash re-entrainment can be described as ash that has already been collected that gets re-directed into the gas stream. Re-entrainment can occur during normal operation duties. The amount of dust re-entrained, compared to the amount of dust not collected in the ESP is extremely difficult to measure (Porle, Francis, & Bradburn, 2005). Rapping losses is a term used by ESP engineers that quantifies the depreciation of collection efficiency during rapping. During rapping dust is dislodged from the discharge and collector electrodes. The amount of free dust in the ESP produced during rapping is much greater than what the ESP has been designed for. Therefore the ESP efficiency will be dramatically reduced during rapping, which increases rapping losses. Continual emission monitoring data indicates the particulate emission level over a required period of time. Figure 2. 4 (bottom graph) indicates the average emission level of 115 mg.Nm^3 during operation where rapping spikes during this period can be noticed.

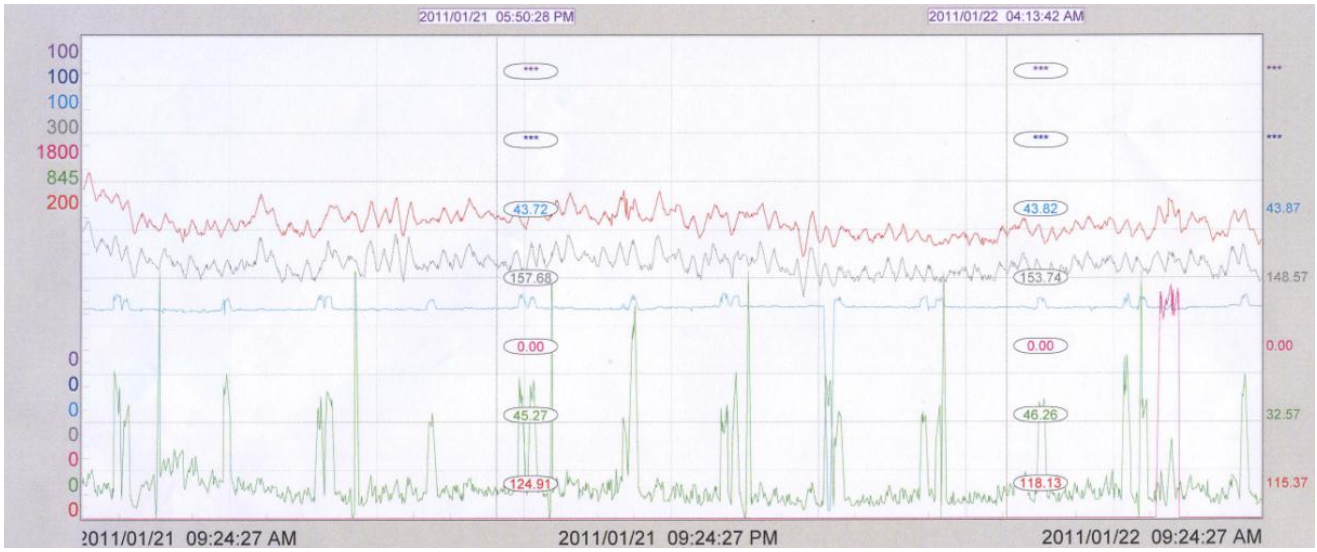

Figure 2. 4: Rapping spikes induced by rapping

Other types of re-entrainment are caused by high velocities, sparking, air ingress, back corona and high hopper levels. It is believed that most particles visible at the stack have been collected once or several times but they were re-entrained and never collected in the ESP (K.R, 1997).

2.14 SPECIFIC COLLECTING AREA (SCA)

The term SCA or Q/A from the Deutsch Equation is an expression which normalises one ESP with another. It indicates the collecting area that is required per m^3/s of flue gas for a desired collection efficiency.

2.15 MIGRATION VELOCITY

Migration velocity describes the speed at which a particle, once charged, migrates towards the collector electrode. The migration velocity is a constant for given operating conditions of a specific local space. It must be noted that the migration velocity is not constant throughout the ESP. The migration velocity varies depending on the conditions of a specific space in the ESP. Parameters like particle size and shape, gas composition, electrical field strength and gas viscosity affects the migration velocity (Kocik, Dekowski, & Mizeraczyk, 2005). The migration velocity cannot be measured; it can only be calculated from the measured ESP efficiency (K.R, 1997). Equation 2.1 indicates the formula to calculate migration velocity.

$$\boldsymbol{\omega} = \frac{\mathbf{EoEpR}}{\mathbf{2\pi\mu}} \qquad (2.\ 1)$$

$\omega = migration\ velocity\ [cm/s]$

$E_0 = strength\ of\ field\ in\ which\ particle\ are\ charged\ [V/m]$

$E_P = strength\ of\ field\ in\ which\ particle\ are\ collected\ [V/m]$

$\mu = dynamic\ gas\ viscosity\ [poise]$

$R = particle\ radius\ [micron]$

2.16 PARTICLE SIZE AND SHAPE

As discussed in chapter 2.3, particle size is mainly determined by the grind ability of the coal and mill settings. Particles migrating through the furnace to the ESP have irregular shapes and sizes. These shapes can vary from spherical, cenospheres, rod shaped, star-like and irregular shapes.

The particles entering the ESP consists of the very small (sub-micron) to the larger (> than 300 μ) sizes and of different shapes, densities and different chemistries (Kim, Park, & Lee, 2001). The ash carried over from a combustion area comprises of a mixture of materials, mainly silica and alumina compounds. These ash particles have a medium particle size of 15μm.

It is known that a large percentage of ash produced in the combustion of a lignite and sub-bituminous coals are sub-micron. Deflagration is a phenomenon that occurs when high percentages of moisture embedded in the coal particles flashes into steam when the particles reach the combustion zone. This results in small explosions that break the coal particles into very fine fragments. The size segment of the resulting ash has a diameter of less than 1 micron. This phenomenon could result in the whole particle size curve shifting with 40 to 55% by weight below the

10 micron level. The primary collection of these small size segments requires operating at optimum levels of voltage and current of the ESP power supplies (Harris, 2003).

Referring to equation 2.1, particle size is a function of the migration velocity. A larger particle has a faster migration and a smaller particle slower migration velocity. Larger particles have more surface area for ions to collide and attach themselves with, therefore there is a stronger force acting on the particle towards the collector electrode, and thus a higher migration velocity.

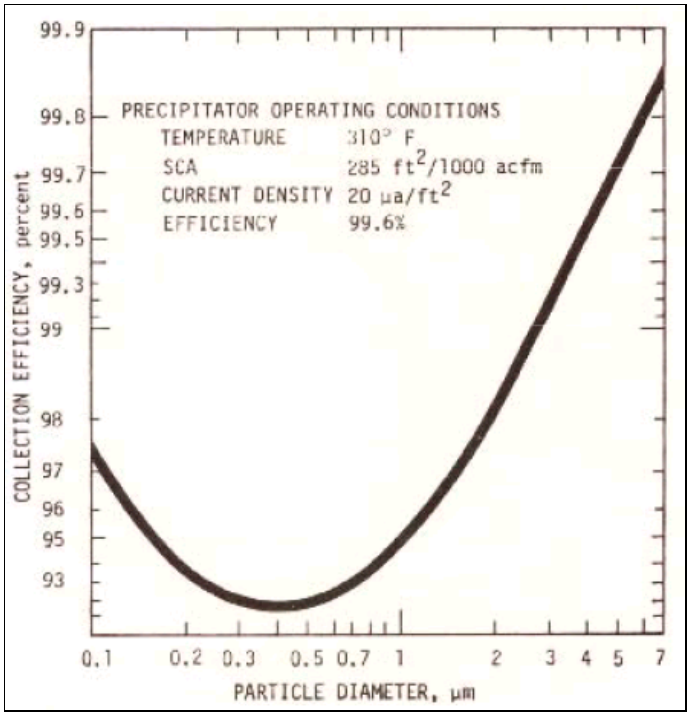

Figure 2. 5: Collection efficiency vs particle diameter (White, 1963)

From the above it is learned that particle size have an effect on the efficiency of an ESP. When developing an ESP simulation model, the model must have the facility to accommodate particle shape and size.

2.17 GAS VISCOSITY

Dynamic viscosity is the property of a fluid that relates shearing stress and fluid motion. At high temperatures the shearing stress is reduced. Viscosity is little dependent on pressure and the effect of pressure can be neglected. As the temperature of water is increased from 60°C to 100°C the density decreases by less than 1%, but viscosity decreased by about 40% (Munson, Young, & Okiishi, 2006). It is thus clear that special attention must be given to temperature when determining viscosity.

An ash particle will therefore move faster through gas with a low viscosity and slower through gas with a high viscosity. Since the migration velocity is dependent on the gas viscosity which is dependent on the gas temperature, is it important to factor these changes in when calculating the migration velocity. An increase in viscosity will decrease the migration velocity while a reduction in viscosity will be beneficial. Viscosity is normally considered in the design phase when looking at the application and location, typical operating temperature and elevation. For example, an ESP operating at 1500m above sea level will need to be sized larger than one running on the same size furnace at sea level. There are usually only minor changes in gas viscosity on a day-to-day basis at any given installation. However, major benefits would accrue for an installation where the gas temperature is not abnormally high (Harris, 2003).

2.18 ESP EFFICIENCY

The most common way to understand the process of electrostatic precipitation is to study the Deutsch-Anderson equation (White, 1963). This equation is globally used by ESP designers and manufactures to determine the theoretical efficiency of the ESP under ideal conditions. The basic form of the equation is given below:

$$\boldsymbol{Efficiency = 1 - e^{-\left(\frac{A\omega}{Q}\right)}} \qquad (2.\ 2)$$

$e = Constant$

$\omega = Migration\ velocity\ (cm/s)$

$A = Effective\ collecting\ plate\ area\ (m^2)$

$Q = Gas\ volume\ flow\ through\ the\ ESP,\ volumetric\ (m^3/s)$

Unfortunately this equation calculates the theoretical efficiency; a number of operating parameters can cause the results to be in error by a factor of more than 2, according to H White (White, 1963). The Deutsch-Anderson equation neglects 3 significant process variables and assumes the following: First, it does not take rapping losses into account. Second, it assumes that all particle sizes and shapes are homogenous, and as a result the migration velocity is the same for all particles in the gas stream. As stated in chapter 2.16, larger particles generally have a faster migration velocity than smaller particles. Third, it assumes the gas flow rate is uniform across the ESP inlet and that particle sneakage through the hopper does not occur (refer to chapter 3.2.6). For the above-mentioned reasons, this equation should only be used for preliminary estimates of ESP collection efficiency.

More accurate predictions on ESP collection efficiency can be obtained by modifying the Deutsch-Anderson equation. This is accomplished by substituting the migration velocity ω with the effective precipitation rate, ω_e. This method is used to calculate preliminary design parameters.

To make the Deutsch-Anderson equation more accurate for cases where all particle sizes are not uniform, the parameter effective-precipitation rate ω_e can be substituted for the migration velocity in equation 2.3 (White, 1963)

Modified Deutsch-Anderson

$$\boldsymbol{Efficiency = 1 - e^{-\left(\frac{A\omega e}{Q}\right)}} \qquad (2.\ 3)$$

$E = Collection\ efficiency\ (\%)$

$e = Constant$

$\omega_e = Effective\ migration\ velocity\ (cm/s)$

$A = Effective\ collecting\ plate\ area\ (m^2)$

$Q = Gas\ volume\ flow\ through\ the\ ESP,\ volumetric\ (m^3/s)$

The difference between the migration velocity ω which refers to the speed at which an individual particle migrates to the collector electrode, the effective precipitation rate ω_e refers to the average speed at which all particles in the gas stream migrates towards the collector electrode. It is important to note that ω_e is calculated from field experience rather than from theory, the values for ω_e are mainly determined by using historical data available from ESP installations or from pilot plant studies.

In conclusion, the effective precipitation rate represents a semi-empirical parameter that can be used to determine the total collection area required for an ESP to operate at a specific collection efficiency to meet a legislative emission limit. Using the modified Deutsch-Anderson equation is beneficial when calculating the additional plate area required during and ESP enhancement project to meet more stringent emission limits. However, operating parameters other than collecting area play a major role in determining the ESP efficiency.

Matts-Ohnfeldt equation

Another modification to the Deutsch-Anderson equation that takes non-ideal parameters into account was derived by Sigvard Matts and Per-Olaf Ohnfeldt in 1962 (White, 1963). The Matts-Ohnfeldt equation reads as follows:

$$\boldsymbol{Efficiency = 1 - e^{-\left(\frac{A\omega k}{Q}\right)^{k}}} \qquad (2.\ 4)$$

E = collection efficiency (%)

e = 2.718282

ω_k = average migration velocity (cm/s)

A = effective collecting plate area (m^2)

Q = gas volume flow through the ESP, volumetric (m^3/s)

K = constant, normally between 0.5 and 1

The term ω_k and ω_e in equation 2.3 and 3.4 are both average migration velocities. The constant k in equation 2.4 is usually between 0.5 and 1 depending on the standard deviation of the particle size distribution and other dust properties affecting the collecting efficiency. Table 2. 4 refer to a study done by Electrostatic Power Research Institute (EPRI) to illustrate the relationship of predicting collection efficiency using the Deutsch-Anderson equation and the Matts-Ohnfeldt equation.

Table 2. 4: Collection efficiency estimations using the Deutsch-Anderson and the Matts-Ohnfeldt equation (Harris, 2003)

Relative size of ESP (A/Q)	Deutsch k = 1.0	Matts-Ohnfeldt		
		k = 0.4	k = 0.5	k = 0.6
1	90	90	90	90
2	99	95.1	96.2	97.2
3	99.9	97.2	98.1	98.8
4	99.99	98.1	99	99.5
5	99.999	98.7	99.6	99.76

When k = 1 the Matts-Ohnfeldt equation is the same as the Deutsch-Anderson equation. To determine the performance of an existing ESP when the gas flow rate varies, using the lower values for k provides more conservative results. From Table 2. 4 one can see the variation in collection efficiency calculated by making use of the two different equations.

When calculating the efficiency of an ESP it is important to identify and select the correct equation that suits your objective and aims.

2.19 ASH RESISTIVITY

According to (Parker, 1997) electrical resistivity of ash is of paramount importance to ESP performance. Electrical resistivity is determined by two mechanisms; volume conductivity, which is a function of the particle matrix constituents, and surface conduction. The latter is governed by the absorbed surface layer, which is related to the surface reactivity and gas components. (Parker, 1997) summarised the effect of ash resistivity on ESP performance as follows: Low resistivity ash is easily charged but loses its charge once it comes into contact with the collector plate. The dust breaks free from the dust layer and is re-entrained into the gas stream. As the resistivity increases under the same charging conditions, the particle arriving at the collector slowly loses its charge and a voltage develops across the dust layer. For a resistivity in the range of 10^{13}ohm.cm and dependent on the dust layer thickness, the voltage reaches a point where positive ions begin to emit from the dust layer. These positive ions cross the inter-electrode spacing and collide with and neutralise negative ions to a point where the precipitation process is effectively diminished (Parker 1997). This condition is known as reversed ionisation or back corona.

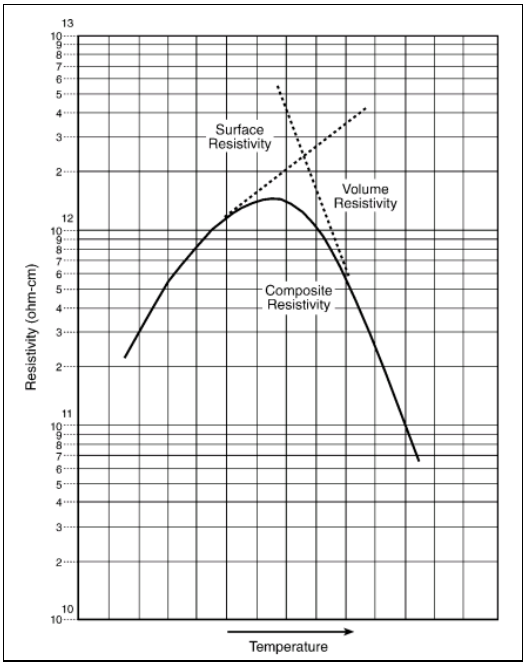

Figure 2. 6: Laboratory measured resistivity curve (Harris, 2003)

Figure 2. 6 represents a resistivity curve of a specific coal with a specific moisture content. Resistivity is very sensitive to moisture content in the ash, the higher the moisture content the lower the resistivity. It is very important to take note of the critical temperature where the resistivity will decrease once past a specific temperature. Some ESP engineers believe that operating an ESP on the other side of the critical point lowers the resistivity back to desired values. They tend to forget all the negative effects associated with high temperatures as mentioned in 2.9. It is therefore important to identify the effect on ESP performance with respect to ash resistivity.

Table 2. 5: Indicates the ranges of different resistivity levels from low resistivity to high resistivity

Resistivity Range	Effect
10^{4} to 10^{7} ohm-cm	Usually highly conductive material - hard to retain - low voltage fields present.
10^{8} to 10^{9} ohm-cm	Sensitive stage where lack of resistive characteristics can sometimes hurt ESP.
10^{10} to 10^{11} ohm-cm	Appears to be the best range to shoot for, should show spark over.
10^{12} to 10^{13} ohm-cm	Range usually associated with < 1% sulfur coals, reduced power in all fields can exist from sparking, difficult range for ESP.
Over 10^{13} ohm-cm	Can produce severe electrical disturbances, or severe back corona.

2.20 CURRENT DISTRIBUTION AND IONIC WIND

It is essential to have proper current distribution, both in the inter-electrode space and along the collecting plates. This enhances the electrical holding forces on the collected particles. Figure 2. 7 illustrate a two-dimensional current distribution along a collecting plate from a discharge electrode with a spike. The current on the collecting plate opposite of the spike is concentrated compared to a section on the collecting without a DE on the opposite side. The current density in this area will also be higher, encouraging particle ionisation. According to (Porle, Francis, & Bradburn, 2005) et al, the reason for this is that the increased electrical field generating the corona is concentrated to the peak while there are other electrical field lines from the body of the specific electrode preventing the current to expand in the space between the electrodes. The corona generation close to a spike distributes over a larger area and the distribution in the inner electrode space and along the collecting plate is more even (Porle, Francis, & Bradburn, 2005).

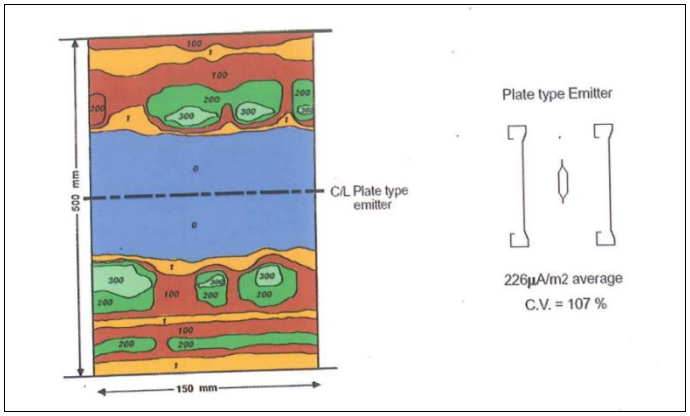

Figure 2. 7: Current distribution along a part of a collecting plate. The number on the plate represents the current density in percentage of the average current density

When considering the ionic wind, ions flowing towards the CE carry gas molecules towards the ion trajectories. This ionic wind becomes stronger as the current density is increased. Gas molecules return to the area where the ionic flow is zero and turbulence is created by the corona current. Figure 2. 8 and Figure 2. 9 The forces acting on the particles caused by the turbulence have various magnitudes and the particles may rather follow the turbulence and become re-entrained without reaching the dust layer (Porle, Francis, & Bradburn, 2005). From a theoretical point of view it would be beneficial to have a gas flow as laminar as possible and the turbulence caused by the protrusions should then be minimised.

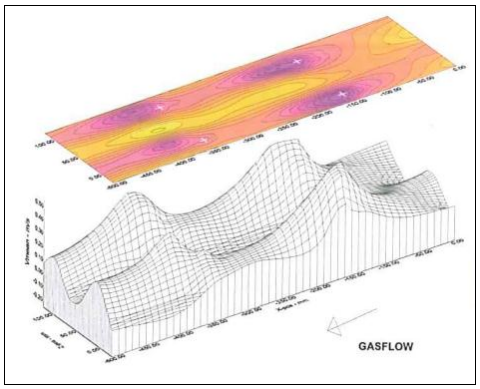

Figure 2. 8: Spiral discharge electrodes

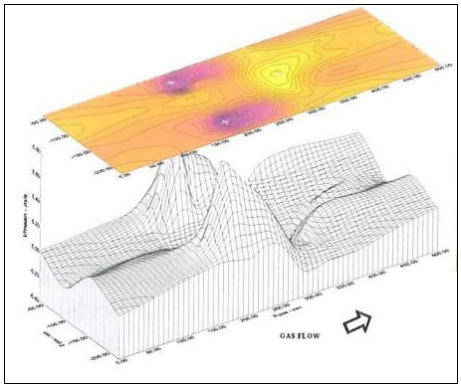

Figure 2. 9: Discharge electrodes with corona peaks

2.21 Electrode alignment, broken or cut electrodes

The alignment between the discharge and collector electrodes is critical to prevent excessive parking between the electrodes, reducing the ESP efficiency. It often happens that the electrodes get damaged or warped during operation, misaligning the electrodes. Alignment between electrodes is important for a constant corona density in the inner electrode space.

Due to the complexity of the ESP design and difficulty to get access to the damaged electrodes, the correct method to get these damaged electrodes replaced or fixed require the ESP roof to be cut open, the damaged electrodes to be hoisted from the ESP casing and replacing them with new electrodes. This is a very timely and costly exercise for little benefit in the overall ESP efficiency. The alternative practice is to cut the damaged and misaligned electrodes. Cutting electrodes reduce the collection efficiency of the specific field, as the collection area will be reduced. On some Eskom power stations more than 30% of one field have been cut out due to warped and damaged electrodes.

2.22 VELOCITY PROFILE

The velocity profile and gas distribution at the inlet of an ESP has a significant effect on the ESP performance. The velocity profile is determined by the inlet cone configuration, turning vane design and primarily by the inlet distribution screens. Usually the distribution screens are a series (usually 3 screens) of perforated plates installed right at the inlet of the ESP. The porosity and location of the holes in the screens determine the velocity profile and the flow distribution through the ESP. Most of the renowned EPS designers and manufactures emphasise the importance of a uniform (all the particles have the same velocity) flow distribution at the ESP inlet. It is also believed that the best ESP performance are achieved with a uniform flow distribution. Figure 2. 10 indicates the effects of

the turning vane design, ESP inlet cone design and the effect on the velocity profile with regards to the distribution screen design.

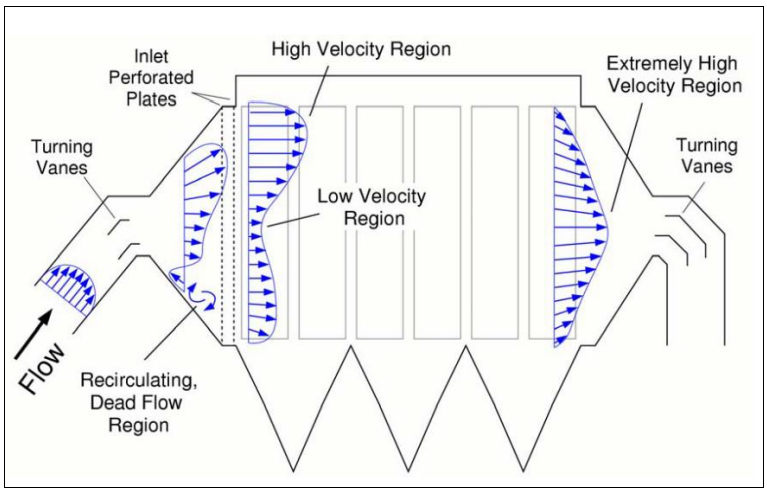

Figure 2. 10: Velocity profile inside the ESP

Some ESP's are equipped with screens at the outlet as well. This is done to manipulate a desired velocity profile other than a uniform profile through the ESP to achieve better EPS performance. This can be contradictory to the above statement. Skew flow is a technique to force the inlet and outlet velocity profiles as indicated Figure 2. 11. CFD technology is used with great success to design the inlet and outlet distribution screens to manipulate uniform flow to skew flow (Schmitz, Pretorious, & Gibson, 1998).

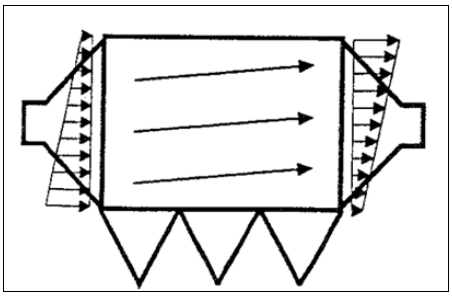

Figure 2. 11: Skew flow inlet and outlet velocity profiles (Hein & Gibson, 1993)

The methodology behind skew flow is described as follows (Hein & Gibson, 1993):

Upper inlet:

This section has a low gas velocity and collects a lower dust load at a higher efficiency. The rapping losses in this section will be high but it applies to a small amount of dust.

Lower inlet:

This section has a higher gas velocity and a higher dust load therefore the efficiency will be lower, but since the dust load is higher more ash will be removed in this section compared to the upper inlet section. Rapping losses are low because the ash is dislodged straight into the hopper.

Upper outlet:

This section has a high velocity with high rapping losses, but receives a low dust burden therefore the losses will be low.

Lower outlet:

This section has a low velocity and therefore high efficiency; the dust burden is high with low rapping losses.

According to (Schmitz, Pretorious, & Gibson, 1998), the implementation of skewed flow at Matimba Power Station has resulted in reducing particulate emission between 50 -70% (Hein & Gibson, 1993). Implementing skewed flow technology has sustainably reduced particulate emissions at various Eskom power stations.

2.23 ESP HOPPER LEVELS

It is very important to note that the hoppers of an ESP are not storage compartments. The hoppers are a component that deals with ash in transit. The hoppers temporarily contain the collected ash and constantly feed the collected ash to the ash handling plant. There are mainly two threads when operating with overfull hoppers. Firstly the build-up of ash inside the hopper can be so severe that the ash starts to penetrate into the ESP electrodes. This scenario causes the fields to trip immediately and could damage the electrodes severely. Secondly, overfull hoppers could cause severe damage to the structure of the ESP. In 2013 Eskom witnessed severe damage to the structure of the ESP due to overfull hoppers. Figure 2. 12 indicates the misalignment of the flanges in relation to the walk-way grid due the structure that has buckled under the weight of the overfull hoppers.

Figure 2. 12: Misaligned flanges

Lastly, overfull hoppers encourage re-entrainment. Overfull hoppers increase the level of the ash by up to 10 meters. Due to this elevated level, the ash is pushed into the main gas stream from where the ash gets re-entrained into the gas stream.

2.24 CONDITION OF ESP

The overall condition of the ESP casing must be in an as-designed state for optimum performance. All inspection doors must be sealed to prevent air ingress. As mentioned earlier, the ESP casing is under a constant vacuum of ± -2 Kpa. Therefore any openings, cracks and holes will cause ambient air to be sucked into the ESP, increasing the volume flow. Air ingress could promote cold spots in certain areas of the ESP that could decrease the temperature to below the acid dew point temperature. Operating below the acid dew point could encrease corrosion on the ESP internals.

2.25 DOWNSTREAM OF THE ESP

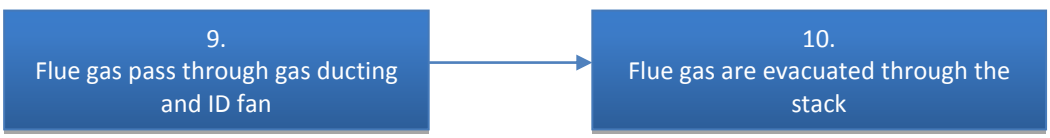

Lastly, the flue gas exits the ESP with little particulate matter in the gas stream. Depending on the ESP condition, one can expect a collection efficiency of 99.9% to 99.8%. The gas ducting between the ESP and the ID fan is also important. Any air ingress in this section could result in an imbalance between the ESP casings. Excessive air ingress could cause the ID fan to run out of capacity, affecting the furnace and casing pressure. From the ID fan onwards and out of the stack there is not much that could have an effect on the ESP performance.

---

3 ESP PARAMETERS AND FUNCTIONING ENHANCEMENTS

3.1 ESP UPSTREAM AND DOWNSTREAM PARAMETERS

For an ESP to operate at its optimum a number of parameters have to be in accordance with design specifications and it must be noted that changes in the various parameters have different effects on the ESP performance.

As mentioned in Chapter 1.1, there are ESP-dependant and ESP-independent parameters. Both the dependent and independent parameters have an effect on the efficiency of an ESP. Dependant parameters form part of the components and design of the ESP. Independent parameters form part of the gas stream properties provided to the ESP. It should be noted when referring to upstream and downstream, the reference point is the ESP inlet.

ESP dependent parameters:

- Collecting plate area
- Discharged electrodes
- Collecting electrodes
- ESP casing
- Power supply
- Control systems
- Rapping philosophy
- Flow distribution screens
- Hopper baffle plates

ESP independent parameters:

Mass flow rate of the flue gas

- Mass flow distribution inside the ESP casing
- Mass flow distribution between the 4 ESP casings
- Velocity distribution inside the casing
- Velocity inside the casing
- ESP inlet temperature
- Ash resistivity
- Partial size
- Particle size distribution
- Ash content
- Furnace and combustion imbalance

The independent parameters are determined by the following aspects:

- Coal quality
- Furnace load
- Pulverised Fuel (PF) fineness
- Combustion air provided to the furnace
- Burner mal distribution
- Deflagration property of the coal (refer to chapter 2.3)
- Burn out time of the coal and flame length
- Furnace leakages
- Furnace and draft group balance
- Soot blowing philosophy
- Air heater blockage and leakages
- SO_3 injection rate
- Condition of guide vanes in the gas ducting

It is worth noting that the input parameters of an ESP is a product of the combustion process and properties of the gas stream as determined upstream of the ESP. It is therefore important to ensure that the inlet conditions of the ESP is as specified. Optimisation of the ESP can only start once all the aforementioned independent parameters meet the specification.

3.2 ESP ENHANCEMENT TECHNOLOGIES

Referring to Table 1. 6, 57% of Eskom's coal fired power stations are equipped with ESP's. Eskom launched various projects to investigate the feasibility of different ESP enhancement technologies. Eskom's research department investigated different ESP enhancement technologies to determine which upgrade options are the most viable to install on Eskom power stations. Different upgrade options have different effects on the ESP and different performance can be expected (Gaikwad & Altman). When selecting an ESP upgrade technology the following criteria are applicable:

- Plant down time
- Capital cost
- Percentage gain in efficiency
- Manufacturing time

The different enhancement technologies available are as follows:

- Reduce the ash resistivity by means of SO_3 injection
- Increase the collecting plate area (Increase the ESP size)
- Improve the discharge electrode design
- Upgrade the ESP energy supply and control systems
- Improve the rapping philosophy
- Improve the ESP inlet flow distribution and reduce sneakage (if fly as pass through the ESP without passing through the energised fields)
- Reduce re-entrainment of dust caused by rapping or high gas velocity
- Change the particle size distribution with agglomeration technologies

Over the past 20 years Eskom managed to reduce particulate emissions by over 70% by installing ESP enhancement technologies. Even with these great achievements some Eskom power stations still do not meet the current emission limits, not to mention the future limits.

It is important to appreciate the fact that Eskom needs to manage its current assets in the ESP's and ensure they are maintained and operated in accordance with the design base. Before any ESP performance enhancement technology can be considered, it is important to ensure the ESP is mechanically and electrically sound and that the upstream conditions (independent variables) are according to specification.

The design specifications for some of Eskom's Power Stations utilising ESP's were not designed for the new legislation requirements. Consequently, some power stations will not be able to achieve the more stringent particulate emission limits.

The different technologies available for improving the performance of an ESP to the required emission levels are (Chambers, 2008):

3.2.1 SO_3 INJECTION

The injection of SO_3 gas into the gas duct before the inlet of the ESP is a technique used to modify and improve the ash resistivity. The resistivity of a particle determines the ease of ionisation and particle charging. The injection rate of SO_3 gas is measured in Parts per Million (ppm) or kg/h. The SO_3 reacts with the H_2O vapour in the flue gas, producing H_2SO_4 (sulphuric acid). The H_2SO_4 gas condensates on the particulates, leaving the particle coated with a layer of sulphuric acid. This layer of H_2SO_4 lowers the particle resistivity which encourages the ionisation properties of the particle and in turn increases the ESP efficiency.

3.2.2 INCREASING THE COLLECTING PLATE AREA (INCREASING THE ESP SIZE)

The term Specific Collecting Area (SCA) (collecting area [m^2] divided by gas flow [m^3/s]) or alternatively A/Q ratio forms part of the Deutsch Equation (equation 2.2) which is used to determine the efficiency of the ESP. In Figure 3. 1 the collector plates have been removed to be replaced with extended collector plates which will increase the collection area and improve the efficiency of the ESP.

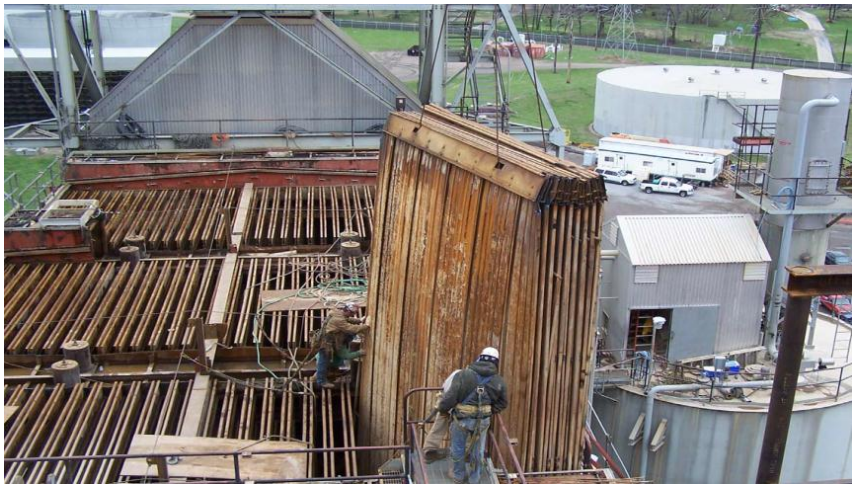

Figure 3. 1: Replacement of discharge and collecting electrodes

3.2.3 IMPROVING THE DISCHARGE ELECTRODE DESIGN

As the technology and associated skills improved since the first ESP's were designed, the design of various ESP components became more advanced. Depending on the type of industry and material collected, it was found that different materials such as pulp, ash and cement have different collection rates depending on the design of the discharge electrode (Arrondel, Bacchiega, & Gallimberti, 2001). It was also determined that the corona formation and current density are heavily affected by the discharge electrode design.

Redesigned discharge electrodes are therefore considered as an ESP enhancement option to improve the performance of the ESP.

3.2.4 UPGRADING THE ESP POWER SUPPLY AND CONTROL SYSTEMS

High frequency (HF) power supply is the latest technology that is being increasingly used in new ESP designs and as an ESP enhancement technology (Bäck, 2006). A HF switched transformer rectifier (TR) produces a smooth high voltage (HV) current compared to conventional TR sets. This HV current is produced at such a high

frequency (50 kHz), the HV current is basically ripple-free. The smooth HV current allows the ESP to operate at a much higher kV and mA that increase the performance of an ESP (Herder & Strydom, 2012)

Eskom has found this ESP enhancement technology as the best option when considering installation time, cost and predicted emission reduction to improve the performance of an ESP. Eskom is currently in a pilot execution phase where HF power suppliers will be installed and tested at Lethabo Power Station.

Figure 3. 2 represent the waveforms at the three different frequencies.

- Orange: 50 Hz with an average field power supply voltage of 60 kV
- Black: 400 Hz with an average field power supply voltage of 70 kV
- Green : 50000 Hz with an average field power supply voltage of 80 kV

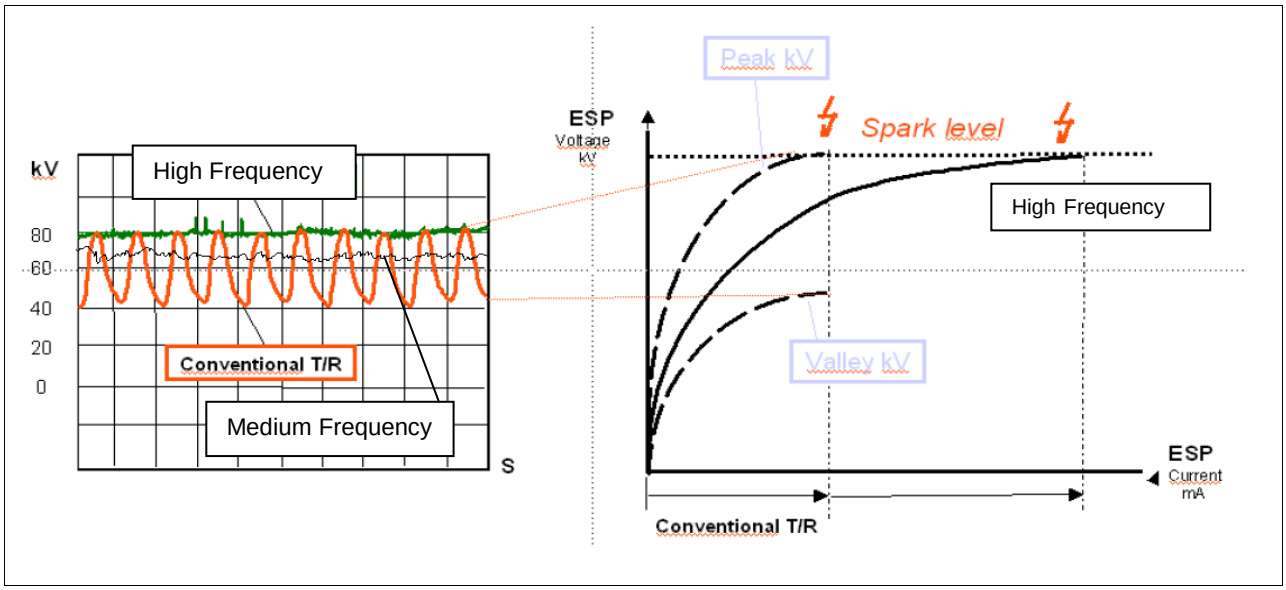

Figure 3. 2: Wave forms of low, medium and high frequency transformers

3.2.5 IMPROVING THE RAPPING PHILOSOPHY

The interval and duration of rapping of the collector and discharge electrodes are determine by the rapping philosophy. This means how frequently which fields will be rapped and for what duration. The less frequent the plates are rapped the thicker the dust layer becomes that develops on the electrodes. This leads to excessive sparking and misalignment of electrodes. Excessive rapping creates unnecessary wear and tear on the components requiring more frequent maintenance.

There is an optimum frequency and duration for the electrodes to be rapped at specific operating conditions. Eskom has achieved great emission reductions by modifying the rapping gearboxes and optimising the rapper timing.

3.2.6 IMPROVING THE ESP INLET FLOW DISTRIBUTION AND REDUCING SNEAKAGE

The inlet cone of an ESP is designed to reduce the duct velocity from 15-20 m/s to 0.8-1.2 m/s. Perforated screens are installed in the inlet cones to produce a more uniform gas distribution over the cross section of the ESP inlet. A more uniform velocity profile ensures that some sections in the ESP are not overloaded with high velocities, reducing the efficiency of that section. High velocity areas also hold the thread of re-entrainment, where ash that has been collected gets re-entrained into the gas stream. Some ESP's are equipped with poorly designed distribution screens or no screens at all. Modern technology like Computational Fluid Dynamics (CFD) has the capacity to design distribution screens to ensure uniform flow at the inlet of the ESP but also to maintain a uniform flow throughout the ESP (Schmitz, et al., 1998). Particle sneakage occurs when the particles flow through the hopper section below missing the electrodes, thus they cannot be ionised and collected. Sneakage is prevented by installing designed baffle plates in the hoppers as indicated Figure 3. 3 (Porle, Francis, & Bradburn, 2005).

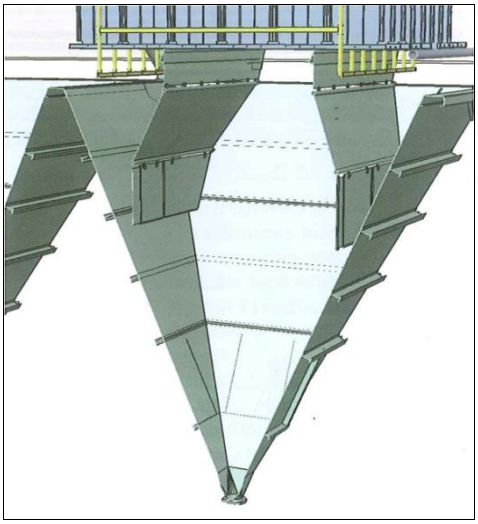

Figure 3. 3: Baffling arrangement in pyramidal hopper

3.2.7 CHANGING THE PARTICLE SIZE WITH AGGLOMERATION TECHNOLOGIES

The injection of ammonia gas into the gas stream is a technique which modifies the particle size entering the ESP. Ammonia injection encourages dust particles to agglomerate developing bigger particles. Chapter 2.16 provides more information on particle size and the effect thereof.

3.3 CONCLUSION ON ESP ENHANCEMENT TECHNOLOGIES

After evaluating the requirements to execute an ESP enhancement project, the following aspects must be noted. Before an enhancement technology can be installed, the ESP must first undergo a General Overhaul (GO). This is to ensure that all the mechanical and electrical components are in an as-designed state. It is important that none of the above-mentioned ESP enhancement technologies can be executed on an ESP which is not mechanically or electrically sound. After a GO the ESP is commissioned to ensure the ESP is in a state to return to service.

With new particulate emission legislation and the consideration of ESP enhancement programs, it is essential to know what emission levels can be achieved by operating the ESP and the furnace at an optimum.

3.4 ESKOM FFP RETROFIT STRATEGY

Bag filters have been found to be the answer to comply with the more stringent legislation. The main advantage of FFP's over ESP's is FFP's are not as process sensitive as ESP's, especially with regards to coal quality. The main process-related concern of FFP's is high furnace back-end temperatures. FFP filtration bags can only withstand temperature of up to 180 °C, thereafter special high temperature bags are required. An FFP is a constant emission filtration plant where an ESP is an efficiency basis plant. Eskom has implemented a FFP retrofit strategy to retrofit all power station equipped with ESP's to FFP's. With the current Eskom capacity constraint conditions it is questionable whether it is possible (and feasible) to retrofit all of the existing ESP installations to FFP's. The main contributing factors are:

It must be noted that this retrofit strategy runs over a period of 15 years, which highlights the fact that some power stations will have to cope with their current emission status for the next 15 years. Considering the above-mentioned, new ways of improving the existing ESP's within the current Eskom environment must be explored.

4 ESP TEST EVALUATION

The data required as inputs for the ESP simulation model can only be measured or tested on site. Some of the data required for this study is measured on a continual basis and is available in the control room. Other data can only be obtained from an ESP efficiency test. An ESP efficiency test is conducted with proper planning and must be executed according to specified standards. The amount of data required and the magnitude of these tests result in it being quite costly and time consuming. An alternative solution to this concern was to investigate results obtained from a previous ESP efficiency test conducted at Lethabo Power Station and determine whether the results could be used for this study. After evaluating the test results of an ESP efficiency test executed in August 2011 at Lethabo Power Station, a decision was made to use the data of that test for this study. Appendix B contains the test report compiled by the contractor (*Inthuu measurements cc*) responsible for the test.

4.1 RESEARCH FACILITIES

Lethabo Power Station is situated in the Vaal Triangle and is a 6 x 600 Mega Watt power station. An ESP efficiency test which formed part of a furnace acceptance test program was executed on unit 2 in August 2011. Each furnace at Lethabo Power Station is equipped with an ESP comprising of 4 parallel casings, namely Left Hand Outer (LHO), left hand inner (LHI), right hand inner (RHI), right hand outer (RHO). Each casing consists of 7 fields which add up to a total of 27 ESP fields.

An ESP efficiency test is performed to provide detailed information on the particulate collection efficiency of an ESP. To calculate the ESP efficiency, measurements must be recorded at the inlet and outlet of the ESP. To determine the total ESP efficiency, the efficiency of each casing must be calculated from the measured data. Therefore, 4 tests need to be executed on the exact same furnace with the same operating conditions. Table 4. 1 indicate some of the important measurements required for this study obtained at the inlet and outlet of the ESP during the ESP test.

Table 4. 1: Data obtained from an ESP efficiency test

Type of measurement	Unit
Gas Temperature	°C
Barometric Pressure	kPa
Duct Pressure	Pa
Oxygen	%
Mass flow rate	Kg/s
Volume flow rate	m^3/s

Table 4. 2: kV and mA reading obtained during the test

LHO1		LHO2		LHO3		LHO4		LHO5		LHO6		LHO7	
Is (mA)	Vs kV)	Is (mA)	Vs kV)	Is (mA)	Vs kV)	Is (mA)	Vs kV)	Is (mA)	Vs kV)	Is (mA)	Vs kV)	Is (mA)	Vs kV)
714.331104	41.9899666	1025.07358	34.3110368	579.591973	27.4147157	645.197324	29.1404682	181.391304	29.8093645	1699.13712	39.5652174	1703.54849	39.1839465
LHI1		LHI2		LHI3		LHI4		LHI5		LHI6		LHI7	
Is (mA)	Vs kV)	Is (mA)	Vs kV)	Is (mA)	Vs kV)	Is (mA)	Vs kV)	Is (mA)	Vs kV)	Is (mA)	Vs kV)	Is (mA)	Vs kV)
225.143813	32.8327759	899.782609	39.3311037	506.183946	46.5585284	558.779264	35.5919732	539.09699	22.4280936	1680.24749	27.1003344	1242.36455	27.0635452
RHI1		RHI2		RHI3		RHI4		RHI5		RHI6		RHI7	
Is (mA)	Vs kV)	Is (mA)	Vs kV)	Is (mA)	Vs kV)	Is (mA)	Vs kV)	Is (mA)	Vs kV)	Is (mA)	Vs kV)	Is (mA)	Vs kV)
767.036789	42.7993311	317.618729	41.2274247	670.826087	45.2307692	375.234114	32.6153846	1235.34114	34.8494983	895.414716	32.0668896	1706.26756	38.3277592
RHO1		RHO2		RHO3		RHO4		RHO5		RHO6		RHO7	
Is (mA)	Vs kV)	Is (mA)	Vs kV)	Is (mA)	Vs kV)	Is (mA)	Vs kV)	Is (mA)	Vs kV)	Is (mA)	Vs kV)	Is (mA)	Vs kV)
963.886288	49.5618729	554.909699	44.3311037	616.729097	31.1270903	1414.40803	53.5451505	1678.32107	47.3277592	1707.32107	42.993311	946.123746	28

Table 4. 2 indicates the power supply readings to the ESP during the ESP efficiency test. Attention was given to the coal quality burned during the test. Coal analysis was done two days before the ESP efficiency test was executed. It was of utmost importance that the batch of coal burned during the test was from the same batch that was analysed 2 days before.

Table 4. 3: Coal analysis of coal burned during test

	Units	
Analytical Moisture	%	**5.50**
Ash	%	**40.70**
Volatile Matter	%	**20.10**
Fixed Carbon (by difference)	%	**33.70**
Fixed Carbon / Volatile Matter		**1.68**
Ultimate Analyses (air dried, % by mass)		
Carbon (Instrument Value)	%	**39.82**
Hydrogen (Instrument Value)	%	**2.50**
Nitrogen	%	**0.89**
Total Sulphur	%	**0.93**
Oxygen (by difference)	%	**9.68**
Hydrogen / Carbon		**0.06**
Gross Calorific Instrument Value	MJ/kg	**15.30**

4.2 TEST EXECUTION

Figure 4.1 represents a top view of four parallel casings. The dark green indicates the measuring location at the inlet of the ESP and the light green indicates the measuring location at the outlet of the ESP.

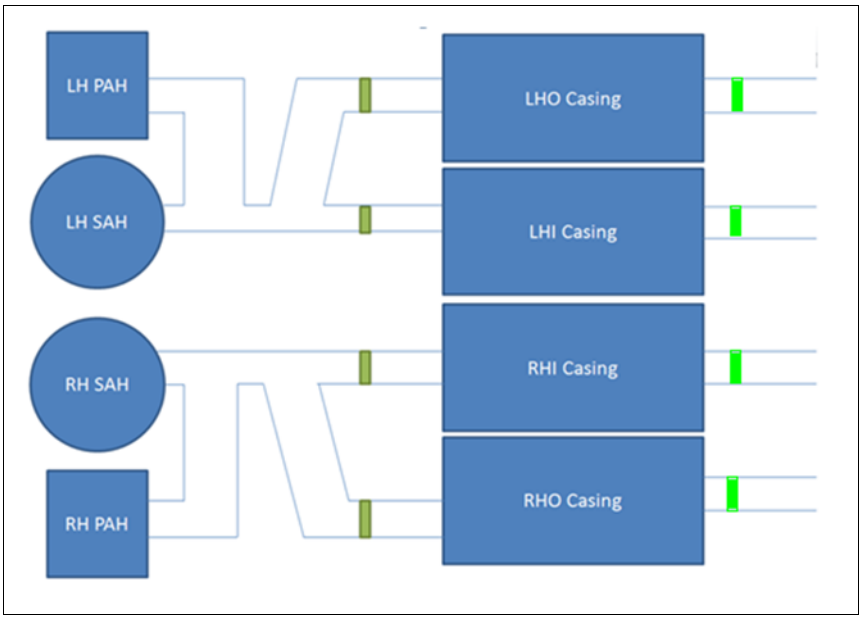

Figure 4. 1: Measuring locations at the inlet and outlet of each casing

One team consisted of three members who were responsible to execute the test. The team set up their equipment on the ESP gas duct ten meters before the ESP inlet and ten meters after the ESP outlet. The ESP gas ducts are designed with four measuring holes over the length of the duct. Four measurements per hole were recorded to compute to sixteen measurements per gas duct (inlet and outlet). This sixteen-point traverse measurement is explained in Figure 5. 5

4.3 DATA GATHERING:

The data gathering was accomplished by means of Isokinetic dust sampling. This is a technique used to determine the dust concentration in a gas stream. A probe connected to a small vacuum pump is inserted into the gas stream. The velocity inside the probe must be equal to the velocity of the gas stream. This is managed by the pump situated on the outside of the duct or pipe. The gas drawn from the gas stream passes through a filter which must be carefully weighed before the test. After a predetermined time with the system in operation, the filter is removed and weighed once more. The gain in weight of the filter is contributed by the particle matter encapsulated in the filter. A mathematical model is then used to determine the dust concentration in the gas stream. The unit for this measurement is mg/Nm^3 or mg/Sm3.

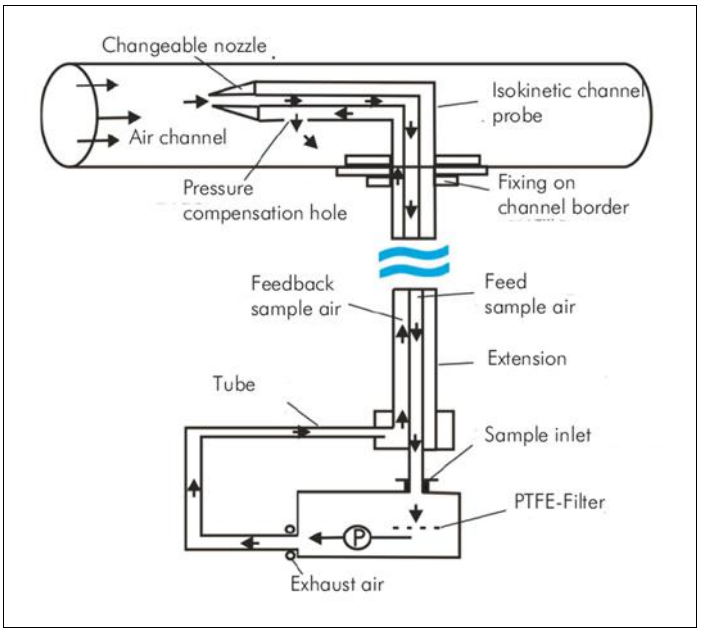

Figure 4. 2: Isokinetic dust sampling

4.4 TEST RESULTS

The results obtained from this test can be viewed in Appendix B. It must be noted that during the test program six ESP efficiency tests were executed. For this study only the measurements from test 1 done on unit 2 on 2011/08/01 from 13H58 to 16H26 were used.

5 COMPILATION OF THE ESP SIMULATION MODEL

An ESP simulation model is developed in Excel to determine the effect of various parameters on the performance of an ESP (This model is tailored for Lethabo Power Station). The model consists of 14 Excel spread sheets. Results calculated in the first sheet feed into the next one and so forth. The sequence of the sheets follows a logical layout that starts with the coal quality and end with the particulate emissions in the stack. The sequence of the spread sheets is as follows:

1. Coal analysis
2. Airflow
3. Total average ideal complete and practical incomplete combustion
4. Left hand right hand combustion
5. Left hand outer and left hand inner calculations (upstream of ESP inlet)
6. Right hand inner and right hand outer calculations (upstream of ESP inlet)
7. ESP size
8. ESP performance
9. Gas viscosity
10. Coal resistivity
11. Left hand outer (downstream of ESP inlet)
12. Left hand inner (downstream of ESP inlet)
13. Right hand inner (downstream of ESP inlet)
14. Right hand outer (downstream of ESP inlet)

Sheets 1 to 6 were developed by Professor C.P Storm. For this study the outputs of sheets 1 to 6 will be used as inputs for the ESP simulation model (sheets 7 to 14).

5.1 CONSTRUCTION OF THE MODEL

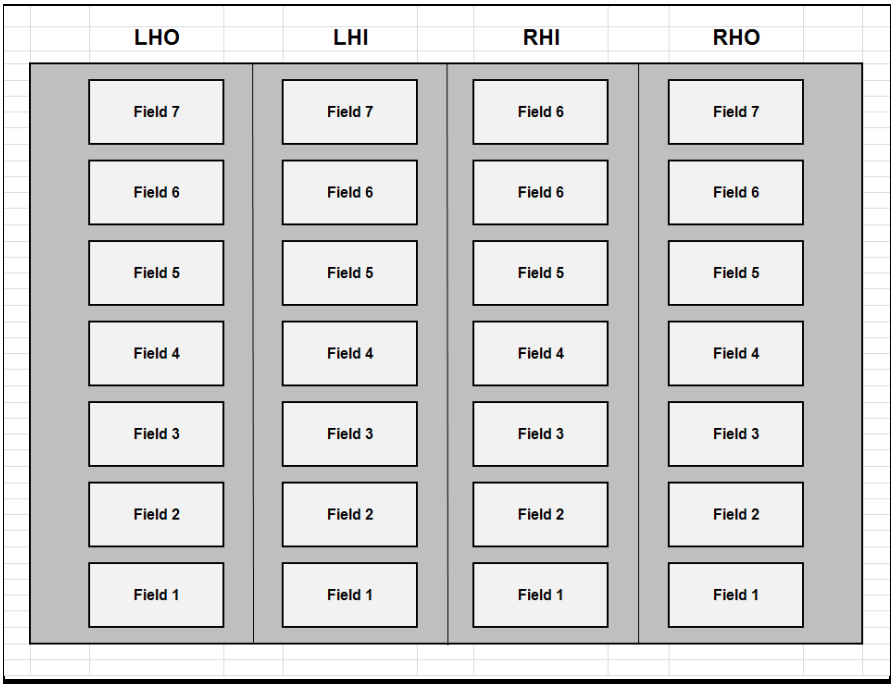

Figure 5. 1: ESP top view, 4 parallel casing 7 field ESP

Figure 5. 1 represents a top view of the ESP layout for Lethabo Power Station. It consists of four parallel casings; LHO, LHI, RHI and RHO. This ESP has seven fields which are each powered by its own rectifier transformer.

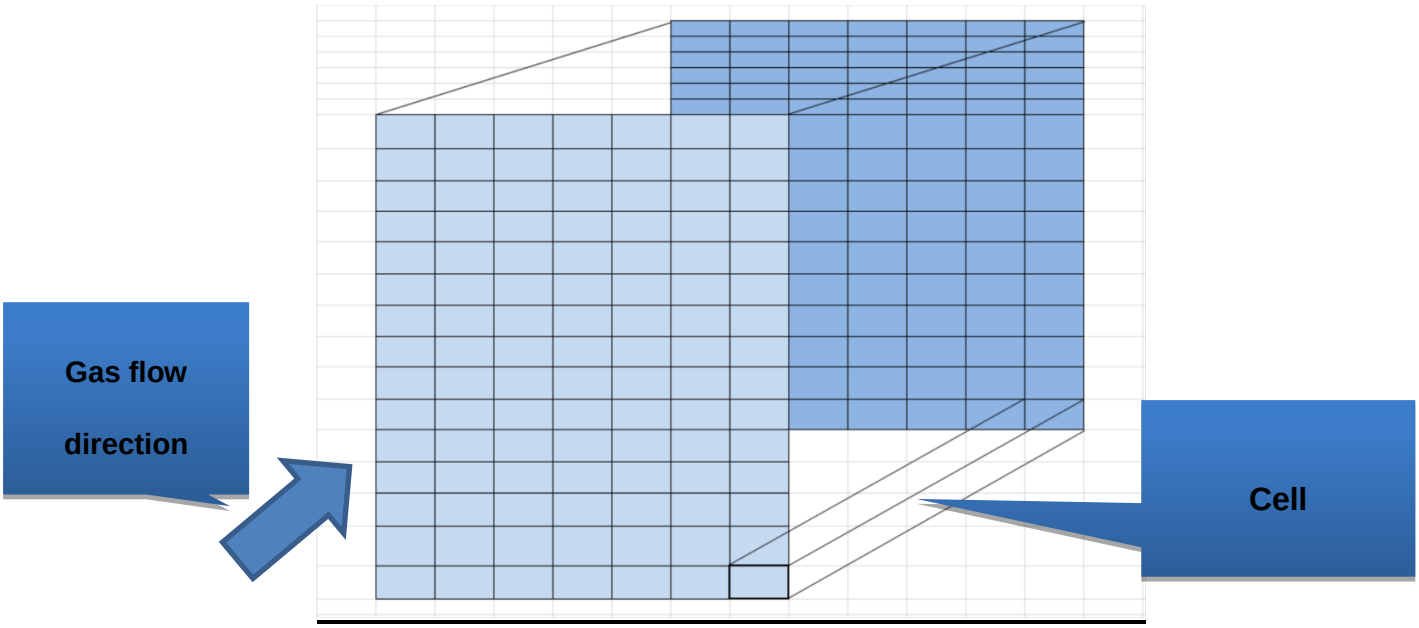

Figure 5. 2: ESP field sectionalised into equally sized cells

Figure 5. 2 represent the method for which the total ESP efficiency is determined. The inlet of each ESP field of each casing is sectionalised into fourteen cells in the field width and fourteen cells in the field height. This computes to a total of 196 equally sized cells for one field. The length of the field is not sectionalised. It is assumed that all the process conditions stay constant though the length of the specific field but conditions can vary for the next fields in line. Each of these cells has its own inputs and variables to calculate the efficiency of the specific cell. The efficiencies for all the cells are averaged to compute the total field efficiency. The weighted average for the seven fields is computed to calculate the total casing efficiency. Based on the volume and mass flow distribution between the four casings, the particulate emissions measured in mg/Nm^3 are calculated for each casing. The particulate emissions for the furnace are calculated from the average of the four ESP casings.

The parameters that can be changed for each cell are:

- Volume flow
- Velocity
- Migration velocity
- Particle size
- Gas viscosity
- Electrical field strength

The following parameters can be changed for each casing:

- Gas Mass flow
- Gas Volume flow
- Gas Temperature
- Ash resistivity
- Gas Velocity

5.2 COAL QUALITY

The coal quality used for this study was measured during the furnace combustion test of August 2011 as well as test conducted in 1997. The approximate and ultimate analyses were obtained from the measurement. The model has the capability to convert the sample type from as-received to air-dried to dry-basis and vice versa by means of the following respective equations 5.1 to 5.3.

As Received to Air-dried:

$$\boldsymbol{Conversion\ factor} = \frac{\mathbf{100}}{(\mathbf{100} - \boldsymbol{Ms_{AR}})} \quad (5.\ 1)$$

$Ms_{AR} = Surface\ moisture\ as\ received$

Air-dried to Dry-basis:

$$\boldsymbol{Conversion\ factor} = \frac{\mathbf{100}}{(\mathbf{100} - \boldsymbol{Mi_{AD}})} \quad (5.\ 2)$$

$Mi_{AD} = Inehrent\ moisture\ air\ dried$

As-received to Dry-basis:

$$\boldsymbol{Conversion\ factor} = \frac{\mathbf{100}}{(\mathbf{100} - \boldsymbol{Ms_{AR}} - \boldsymbol{Mi_{AD}})/((\mathbf{100} - \boldsymbol{Ms_{AR}})(\mathbf{100}))} \quad (5.\ 3)$$

Table 5. 1: Coal conversion: As received to Air dried to Dry basis

CONVERSION BASED ON INITIAL M_s (AS RECIEVED), M_i (AIR DRIED), VOLATILES & ASH (DRY BASIS), C_{FIXED} BY DIFFERENCE (DRY BASIS):						
Sample type:			**AS RECEIVED**		**AIR Dried**	**Dry Basis:**
Conversion:			As Received from Air Dried	As Received from Dry Basis	Air Dried from Dry basis	Dry Basis: **Given**
Conversion formula:			100/(100-$M_{s\ AR}$)	100/(100 - $M_{s\ AR}$ - MI_{AD} / ((100-$M_{s\ AR}$)*100))	100/(100-$M_{i\ AD}$)	
Conversion factor:			1.0488	1.086	1.0352	
GRAVIMETRIC %	**SYMBOL**	**UNITS**	Corrected	Corrected	Corrected	Corrected
Carbon $_{Fixed}$ (by difference)	C_{FIX}	%	32.896	32.896	34.500	**35.714**
Volatile matter	VM	%	16.972	16.972	17.800	**18.427**
Ash	Ash	%	42.240	42.240	44.300	**45.859**
Surface moisture	M_s	%	**4.650**	4.650	0.000	0.000
Inherent moisture	M_i	%	3.242	3.242	**3.400**	0.000
Total moisture	M_t	%	7.892	7.892	3.400	0.000
Gross calorific value	GCV_v	[MJ/kg]	14.016	14.016	14.700	**15.217**
Total			100.000	100.000	100.000	100.000

COAL ANALYSIS CONVERSION						
ULTIMATE ANALYSIS						
CONVERSION BASED ON INITIAL M_s (AS RECIEVED), M_i (AIR DRIED), N, O (by difference), C_{Tot}, ASH, S, H (DRY BASIS):						
Sample type:			**AS RECEIVED**		**AIR Dried**	**Dry Basis:**
Conversion:			As Received from Air Dried	As Received from Dry Basis	Air Dried from Dry basis	Dry Basis: **Given**
Conversion formula:			100/(100-$M_{s\ AR}$)	100/(100 - $M_{s\ AR}$ - MI_{AD} / ((100-$M_{s\ AR}$)*100))	100/(100-$M_{i\ AD}$)	
Conversion factor:			1.0488	1.086	1.0352	
GRAVIMETRIC %	**SYMBOL**	**UNITS**	Corrected	Corrected	Corrected	Corrected
Nitrogen	N	%	0.820	0.820	0.860	**0.890**
Oxygen (by difference)	O	%	7.363	7.363	7.722	**7.993**
Carbon $_{Total}$	C_{Tot}	%	37.635	37.635	39.470	**40.859**
Ash	A	%	42.240	42.240	44.300	**45.859**
Sulphur	S	%	1.478	1.478	1.550	**1.605**
Hydrogen	H	%	2.573	2.573	2.698	**2.793**
Surface Moisture	M_s	%	**4.650**	4.650	0.000	0.000
Inherent Moisture	M_i	%	3.242	3.242	**3.400**	0.000
Total moisture	M_t	%	7.892	7.892	3.400	0.000
Total			100.000	100.000	100.000	100.000

Table 5. 1 indicates the 3 columns of the basis of the coal. Note the correction factors computed equations 5.1 to 5.3.

5.3 COAL FEED RATE

The coal feed rate is mainly dependent on the boiler load and can be obtained from the control room. The total coal flow rate is determined by the sum of the flow rates of all the coal feeders, measured in m^3/h.

$$\sum(\boldsymbol{Feeder\ flow\ rate}) \tag{5. 4}$$

The model converts m^3/h to kg/s with bulk density:

$$\sum(\boldsymbol{Feeder\ flow\ rate})/\boldsymbol{3.6} \tag{5. 5}$$

5.4 TOTAL AIR SUPPLIED TO FURNACE

The stoïchiometric air required to combust coal to produce CO_2, O_2, NO_2, H_2O, SO_2 is calculated as indicated in Table 5. 2

Table 5. 2: Chemical reactions for stoïchiometric combustion

CHEMICAL REACTIONS								
IDEAL COMPLETE COMBUSTION					PRACTICAL INCOMPLETE COMBUSTION			
C	+	O_2	=	CO_2	2C	+	O_2	=	2CO
12.011		31.999		44.010	24.022		31.999		56.021
1.000		2.664		3.664	1.000		1.332		2.332
37.635		100.263		137.898	37.179		49.525		86.704
					2CO	+	O_2	=	$2CO_2$
					56.021		31.999		88.020
					1.000		0.571		1.571
					86.704		49.525		136.229
					86.640		49.488		136.128
S	+	O_2	=	SO_2	S	+	O_2	=	SO_2
32.060		31.999		64.059	32.060		31.999		64.059
1.000		0.998		1.998	1.000		0.998		1.998
1.478		1.475		2.953	1.478		1.475		2.953
$2H_2$	+	O_2	=	$2H_2O$	$2H_2$	+	O_2	=	$2H_2O$
4.032		31.999		36.030	4.032		31.999		36.030
1.000		7.937		8.937	1.000		7.937		8.937
2.573		20.421		22.994	2.573		20.421		22.994
					N_2	+	$2O_2$	=	$2NO_2$
					28.013		63.998		92.011
					1.000		2.285		3.285
					0.133		0.303		0.435

The total air supplied is calculated from the measuring aerofoil measurements by means of the ΔP method ($P_{STAG} = P_{STAT} + P_{DYN}$), from which the velocity is calculated. The mass flow is calculated with the velocity, the duct cross-sectional area, the density, and a pre-determined Cd factor (Du Toit, 1991). The wet and dry bulb temperatures are used to calculate the relative and absolute humidity, to produce the amount of moisture in the air supplied. This is subtracted from the air supplied to render the dry air only, which participates in combustion.

Once this net combustion air is determined, taking into account the measurable in-leakages such as mill seal air and burner core air, the excess air can be determined. The air heater leakage and un-measurable furnace in-leakage is determined by means of iterations with the Excel "goal seek" function. Correlations are done with the measured burner, economiser outlet and airheater outlet O_2%, as well as with CO_2%, and correlated with the Ostwald diagram principle Figure 5. 3. The y axis represents the CO_2% and the X axis the O_2%. All these gas analysis calculations are done for gravimetric wet as well as volumetric dry gas composition (the latter being the basis of the gas analyser measurement).

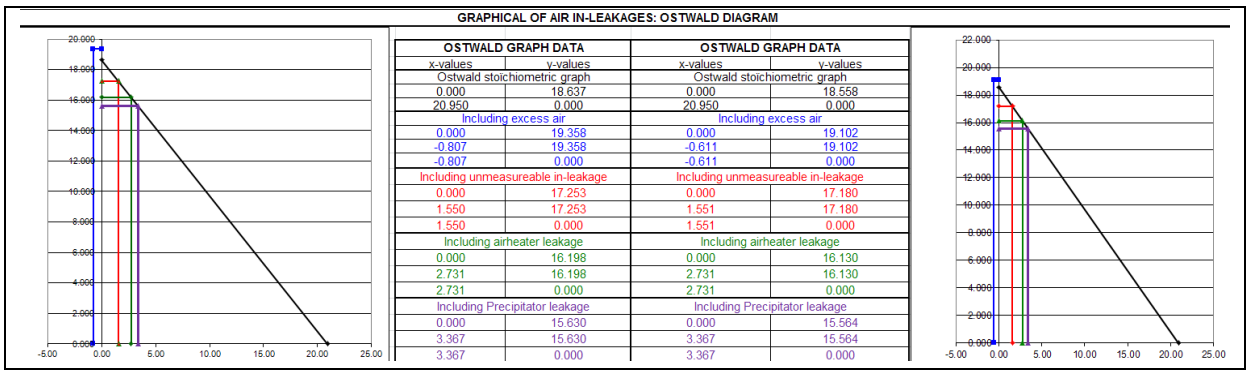

Figure 5. 3: Ostwald diagram

In the Ostwald diagram the stoïchiometric (black), the excess air (blue), the furnace in-leakage (red), the airheater leakage (green) and the ESP leakage (purple) relationships can be seen. The gas constituents namely CO_2, H_2O, N_2, O_2, CO, NO_x and SO_2 are calculated (gravimetric wet and volumetric dry) at the burner outlet, economiser outlet, air heater outlet, ESP inlet and ESP outlet. The sum of all the constituents equates the total flue gas mass flow (kg/s) at the burner outlet, economiser outlet, air heater outlet, ESP inlet and ESP outlet.

5.5 TOTAL FLUE GAS VOLUME FLOW

The gas volume flow is calculated by using equation 5.7. The volume flow is calculated for various process conditions at the burner outlet, economiser outlet, air heater outlet, ESP inlet and ESP outlet.

$$\boldsymbol{PV} = \dot{m}\boldsymbol{RT} \tag{5. 6}$$

$$\boldsymbol{V} = \frac{\dot{m}\boldsymbol{RT}}{\boldsymbol{P}} \tag{5. 7}$$

$\dot{m}$ = *Mass flow [kg/s]*

V= Volume flow [m^3/s]

R= Gas constant [kJ/kg-K]

T= Temperature [Kelvin]

P= Pressure [kPa]

The total volume flow split into the right hand and left hand side of the furnace calculated from the air heater leakage, duct pressures and gas temperatures. After the left hand and right hand air heaters the volume flow is again split into two to calculate the volume flow for the LHO,LHI,RHI and RHO ESP casings.

5.6 TOTAL DUST BURDEN

The ash flow rate, measured in kg/s, is a function of the coal feed rate and the percentage ash in the coal.

$$\boldsymbol{Ash\ flow\ rate} = (\boldsymbol{coal\ feed\ rate})(\%\ \boldsymbol{ash\ in\ coal}) \tag{5. 8}$$

Depending on the bottom to top ash ratio, the ash flow rate is multiplied by the top ratio to accommodate for the ash directly falling down into the ash hopper. This is

usually the heavier and agglomerated particles. Equation 5.9 is used to determine the particulate emission measured in mg/Am^3 evacuated to the four ESP casings

$$\boldsymbol{Dust\ burden\ from\ furnace} = \frac{\boldsymbol{total\ ash\ flow\ rate}}{\boldsymbol{total\ volume\ flow\ rate}} \quad (5.\ 9)$$

The dust burden for a specific casing is calculated by dividing the ash flow rate of the casing by the volume flow of the casing as indicated in equation 5.10

$$\boldsymbol{Dust\ burden\ casing} = \frac{\boldsymbol{(Mass\ flow\ rate\ casing)(1000)}}{\boldsymbol{Volume\ flow\ rate\ casing}} \quad (5.\ 10)$$

5.7 AIR HEATER PERFORMANCE

It is important to accommodate the air heater performance. Figure 5. 4 explains the flow diagram of the air and flue gas. It must be noted that the percentage air heater leakage indicated by the red line must be added to the total gas volume flow. Referring to equation 5.10, it is important to calculate the correct volume flow that will pass through the ESP.

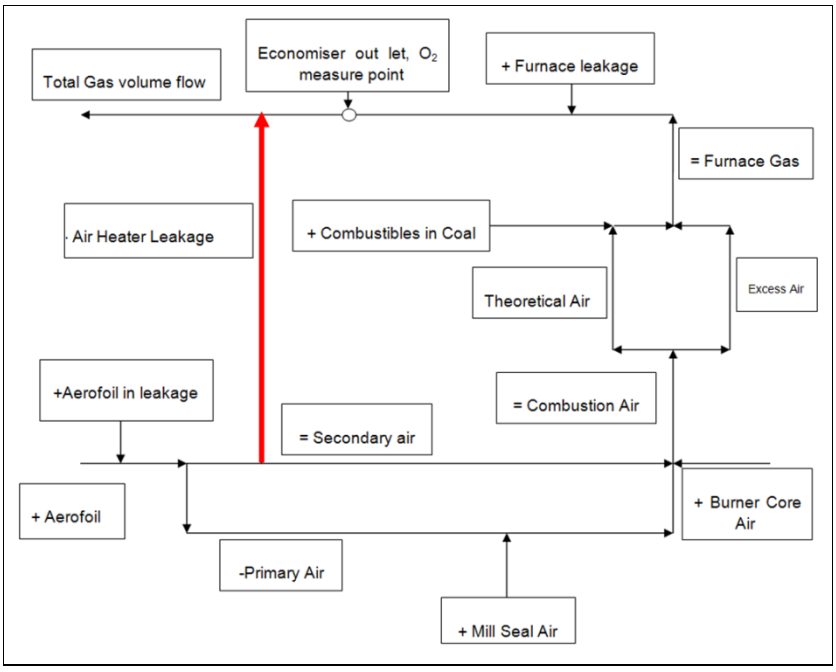

Figure 5. 4 : Air leakage into flue gas due to air heater leakages (Storm, 1998)

5.8 FLUE GAS TEMPERATURE

The flue gas temperature is measured by means of a 16-point traverse mesh in each of the four ducting's towards the ESP. The average of these sixteen measurements serves as the input value for the temperature of each ducting. The accuracy of these measurements is crucial since the ash resistivity, gas volume flow and gas viscosity are governed by the temperature. Equation 5.6 to verify the answers obtained for measurements.

5.9 FLUE GAS VELOCITY AND VELOCITY DISTRIBUTION

The gas velocity in the ESP casing is very difficult to measure during operation, the reasons for this being access for measuring devices and electrocution risks. It is assumed that the flue gas velocity is constant throughout the entire ESP from inlet to outlet. As indicated in chapter 4, the velocity and temperature was measured at the ESP ducting towards the ESP. During the test, data was obtained from a 16-point traverse measurement. Figure 5. 5 indicates the test location on the ESP duct where the measurements were taken. The assumption is that the data obtained from the traverse test in the ESP duct will correspond to an equivalent 16-point mesh in the ESP casing. The readings of the measurements in each of the 16 cells are multiplied by a factor (equation 5.13) to determine the corresponding values for each of the 16 cells at the ESP inlet. The values calculated for the ESP inlet is used as input values for the ESP simulation model.

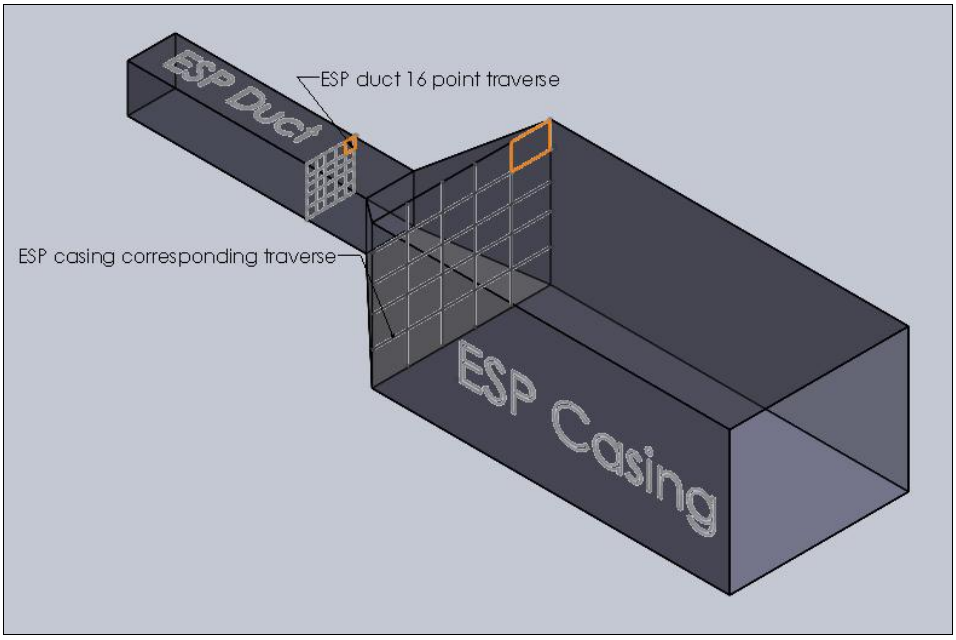

Figure 5. 5: 16-Point traverse in ESP duct and ESP casing

Figure 5. 5 illustrate how the velocity input values are obtained from the measurements taken at the ESP ducting. The orange cells indicate how the measurement from the ESP duct corresponds to the velocities determined for the ESP inlet. By means of equation 5.13 the velocity at the ESP inlet is calculated for each cell.

$$\boldsymbol{Q_i = Q_1} \tag{5.11}$$

$$\boldsymbol{V_i A_i = V_1 A_1} \tag{5.12}$$

$$\boldsymbol{V_1 = \frac{Vi\ Ai}{A1}} \tag{5.13}$$

Q_i= Volume flow duct [m^3/s]

Q_1 = Volume flow ESP [m^3/s]

V_i= Gas velocity duct [m/s]

V_1 = Gas velocity ESP [m/s]

A_i= Area duct [m^2]

A_1 = Area ESP [m^2]

5.10 MIGRATION VELOCITY

The migration velocity is calculated by means of equation 5.14. The average of the charging electric field and the collecting electric field were determined in the middle of the discharge and collector electrode..

$$\boldsymbol{\omega = \frac{EoEpA}{2\pi\mu}} \tag{5.14}$$

Eo = Charging electric field

Ep = Collecting electric field

A = Particle radios

μ = Flue gas viscosity

5.11 GAS VISCOSITY

Engineering Equation Solver (EES) was used to calculate the gas viscosity. The viscosity of each of the gas constituents namely CO_2, H_2O, N_2, O_2, CO, NO_2 and SO_2 is calculated in a temperature range from 90°C to 250°C. EES provides the user with a second order polynomial equation for each of the gas constituents. These equations are a function of the flue gas temperature.

The total flue gas viscosity is calculated by the weighted average of each of the gas constituents obtained from the combustion calculations.

$$\mu gas = \frac{((CO2 * 20.929) + (CO * 0.021) + (SO2 * 0.147) + (NO2 * 0.092) + (O2 * 3.846) + (H2O * 5.564) + (N2 * 69.401))}{100}$$

A second order polynomial equation is derived from the weighted gas viscosity (μ_{GAS}). This equation is a function of temperature; therefore the viscosity of the flue gas can be determined at any temperature between 90°C to 250°C.

5.12 GAS PRESSURE

Equation 5.6 was used to calculate the gas pressure. The pressure is calculated for various process conditions at the burner outlet, economiser outlet, air heater outlet, ESP inlet and ESP outlet.

5.13 ESP EFFICIENCY

The Matts-Ohnfeldt equation is used to calculate the efficiency of the ESP. It is very important to distinguish between equations 5.15 and equation 5.16.

It reads as follows:

$$\boldsymbol{Efficiency = 1 - e^{-\left(\frac{A\omega k}{Q}\right)^{k}}} \quad (5.15)$$

$$\boldsymbol{Efficiency = 1 - \frac{1}{e^{(A\omega k/Q)k}}} \quad (5.16)$$

E = collection efficiency (%)

e = 2.718282

ω_k = average migration velocity (cm/s)

A = effective collecting plate area (m^2)

Q = gas volume flow through the ESP, volumetric (m^3/s)

K = constant, normally between 0.5 and 1

Equation 5.15 is used to determine the efficiency (%) of ash that is collect in the ESP. Equation 5.16 is used to determine the efficiency (%) of ash not collected in the ESP as indicated in Figure 5. 6

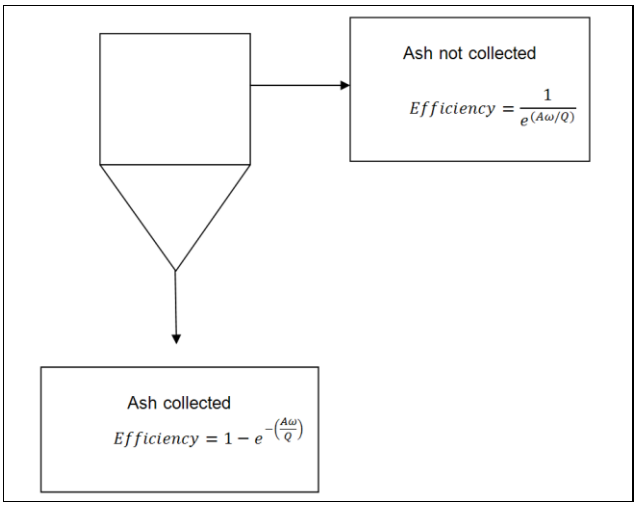

Figure 5. 6: Deutsch−Anderson equation in two different forms for ash collected and ash not collected

The model makes use of equation 5.16 to calculate the dust burden that will exit the ESP and not the dust burden collected in the hoppers.

5.14 PARTICULATE EMISSIONS

The outlet dust burden of each field is calculated based on the efficiency of the respective field and the inlet dust burden of the respective field. The outlet dust burden of field 7 for all of the four casings is averaged to provide the total particulate emission measured in mg/Nm^3. Figure 5.7 demonstrates the logic of the system.

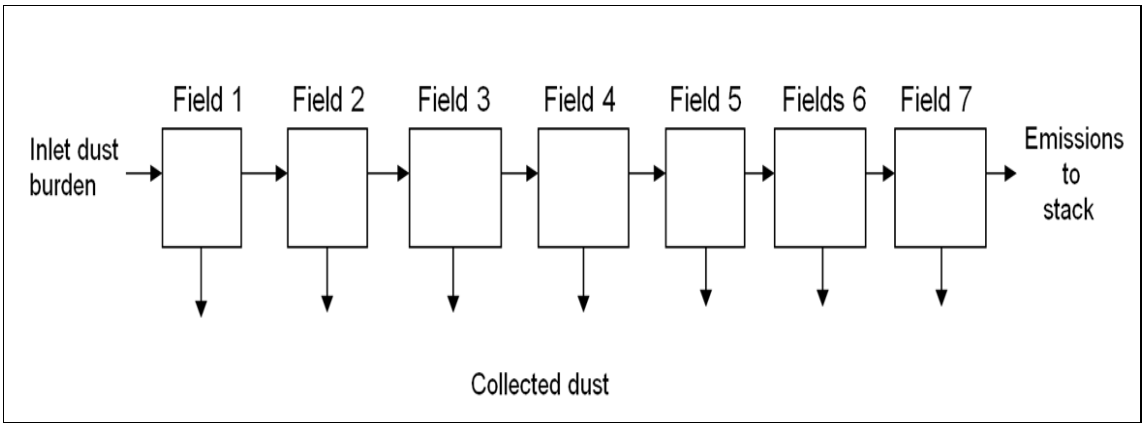

Figure 5. 7: Logical layout of how the total ESP efficiency is determined.

5.15 GAS DENSITY

EES was used to calculate the gas density. The density of each of the gas constituents namely CO_2, H_2O, N_2, O_2, CO, NO_2 and SO_2 is calculated in a temperature range from 90°C to 250°C. EES provides the user with a second order polynomial equation for each of the gas constituents. These equations are a function of the flue gas temperature.

$$\rho\_Gas\_[i] = \frac{((CO2 * 20.929) + (CO * 0.021) + (SO2 * 0.147) + (NO2 * 0.092) + (O2 * 3.846) + (H2O * 5.564) + (N2 * 69.401))}{100}$$

A second order polynomial equation is derived from the weighted gas density (ρgas). This equation is a function of temperature; therefore the density of the flue gas can be determined at any temperature between 90°C to 250°C

5.16 CORRECTION FACTOR FOR SO_3 CONDITIONING

The ESP simulation model does not take the amount of SO_3 injected into account. It is experienced that the only mathematical equation, developed by R.E Bickelhaupt, available to calculate coal resistivity is not applicable to South African coals (Bickelhaupt, 1979). Thus to calculate the effect on ash resistivity with regards to SO_3 injection is very difficult and therefore excluded from this study. To accommodate for the injection of SO_3, the results obtained from an engineering study for Lethabo Power Station was used. Eskom contracted EPRI (Electric Power Research institute) to determine the possible reduction in particulate emissions when considering SO_3 injection. The results indicated that the particulate emission at Lethabo Power Station could be reduced by 56% if 20 ppm of SO_3 gas is injected into the flue gas stream (Bosch, 1998). To accommodate for the effect of SO_3 injection the final calculated dust burden at the outlet of the ESP is multiplied by a correction factor of 56%.

5.17 ASH RESISTIVITY

The input parameters for ash resistivity are obtained from laboratory tests conducted over the same period as the furnace combustion test. The excel spread sheet makes use of a look-up function to determine the resistivity at the corresponding temperature.

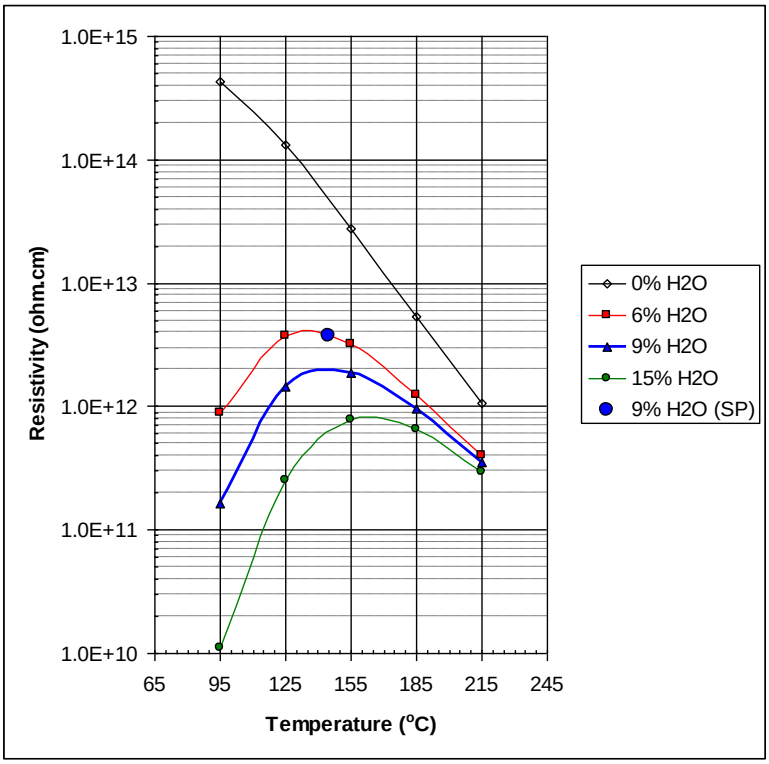

Figure 5. 8: Laboratory resistivity curves for 4 different moisture contents

5.18 ELECTRICAL FIELD STRENGTH

The electrical field strength is measured in kV/cm. The field strength weakens the further away from the discharge electrode. It must be noted that the lane spacing for Lethabo Power Station is 300 mm. Therefore the distance between the discharge and collector electrode is 150 mm. The distance used in the model is 75 mm which is the middle of the lane between the collector and discharge electrode. The electrical field strength is determined by dividing the supplied voltage (kV) by 7.5 cm.

5.19 BROKEN OR CUT ELECTRODES

To determine the loss in efficiency due to broken or cut electrodes, the user must determine the actual surface area lost by means of inspection. The surface area lost is converted to a percentage of the total surface area. If, for argument's sake, only 20% of the total surface area is removed, 80% of the field is in operation. As indicated in previously the inlet of each field is meshed into 196 blocks. To accommodate for the 20% loss in surface area, 20% of the 196 blocks are zeroed. Therefore the contribution of the 20% in surface area will be disregarded in the total field efficiency. Figure 5.9 illustrates exactly how the 20% of the total surface area are zeroed for one ESP field.

Velocity in each sell													
1.280	1.280	1.280	1.280	1.280	1.280	1.280	1.280	1.280	1.280	1.280	1.280	1.280	1.280
1.280	1.280	1.280	1.280	1.280	1.280	1.280	1.280	1.280	1.280	1.280	1.280	1.280	1.280
1.280	1.280	1.280	1.280	1.280	1.280	1.280	1.280	1.280	1.280	1.280	1.280	1.280	1.280
1.280	1.280	1.280	1.280	1.280	1.280	1.280	1.280	1.280	1.280	1.280	1.280	1.280	1.280
1.280	1.280	1.280	1.280	1.280	1.280	1.280	1.280	1.280	1.280	1.280	1.280	1.280	1.280
1.280	1.280	1.280	1.280	1.280	1.280	1.280	1.280	1.280	1.280	1.280	1.280	1.280	1.280
1.280	1.280	1.280	1.280	1.280	1.280	1.280	1.280	1.280	1.280	0.000	0.000	0.000	0.000
1.280	1.280	1.280	1.280	1.280	1.280	1.280	1.280	1.280	1.280	0.000	0.000	0.000	0.000
1.280	1.280	1.280	1.280	1.280	1.280	1.280	1.280	1.280	1.280	0.000	0.000	0.000	0.000
1.280	1.280	1.280	1.280	1.280	1.280	1.280	1.280	1.280	1.280	0.000	0.000	0.000	0.000
1.280	1.280	1.280	1.280	1.280	1.280	1.280	1.280	1.280	1.280	0.000	0.000	0.000	0.000
1.280	1.280	1.280	1.280	1.280	1.280	1.280	1.280	1.280	1.280	0.000	0.000	0.000	0.000
1.280	1.280	1.280	1.280	1.280	1.280	1.280	1.280	1.280	1.280	0.000	0.000	0.000	0.000
1.280	1.280	1.280	1.280	1.280	1.280	1.280	1.280	1.280	1.280	0.000	0.000	0.000	0.000

Figure 5.9: 20 % of the 196 cells are zeroed, resulting in 20% loss in surface collecting area

5.20 EFFECT OF VELOCITY PROFILE

To accommodate for various velocity profiles the user can manipulate the velocity input sheet to adopt a desired velocity profile. The input values are manually inserted, to develop the velocity profile indicated on the left hand side of the Figure 5. 10

In let velocity profile

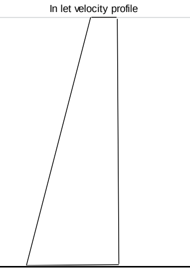

Velocity in each sell													
0.700	0.700	0.700	0.700	0.700	0.700	0.700	0.700	0.700	0.700	0.700	0.700	0.700	0.700
0.800	0.800	0.800	0.800	0.800	0.800	0.800	0.800	0.800	0.800	0.800	0.800	0.800	0.800
0.900	0.900	0.900	0.900	0.900	0.900	0.900	0.900	0.900	0.900	0.900	0.900	0.900	0.900
1.000	1.000	1.000	1.000	1.000	1.000	1.000	1.000	1.000	1.000	1.000	1.000	1.000	1.000
1.100	1.100	1.100	1.100	1.100	1.100	1.100	1.100	1.100	1.100	1.100	1.100	1.100	1.100
1.200	1.200	1.200	1.200	1.200	1.200	1.200	1.200	1.200	1.200	1.200	1.200	1.200	1.200
1.300	1.300	1.300	1.300	1.300	1.300	1.300	1.300	1.300	1.300	1.300	1.300	1.300	1.300
1.400	1.400	1.400	1.400	1.400	1.400	1.400	1.400	1.400	1.400	1.400	1.400	1.400	1.400
1.500	1.500	1.500	1.500	1.500	1.500	1.500	1.500	1.500	1.500	1.500	1.500	1.500	1.500
1.600	1.600	1.600	1.600	1.600	1.600	1.600	1.600	1.600	1.600	1.600	1.600	1.600	1.600
1.700	1.700	1.700	1.700	1.700	1.700	1.700	1.700	1.700	1.700	1.700	1.700	1.700	1.700
1.800	1.800	1.800	1.800	1.800	1.800	1.800	1.800	1.800	1.800	1.800	1.800	1.800	1.800
1.900	1.900	1.900	1.900	1.900	1.900	1.900	1.900	1.900	1.900	1.900	1.900	1.900	1.900
2.000	2.000	2.000	2.000	2.000	2.000	2.000	2.000	2.000	2.000	2.000	2.000	2.000	2.000

Figure 5. 10: Velocity distribution at the inlet of a field to accommodate the velocity profile on the left hand side of the figure.

CFD simulation results could be used as inputs for this sheet to determine the effect of various velocity profiles of ESP performance.

5.21 PARTICLE SIZE

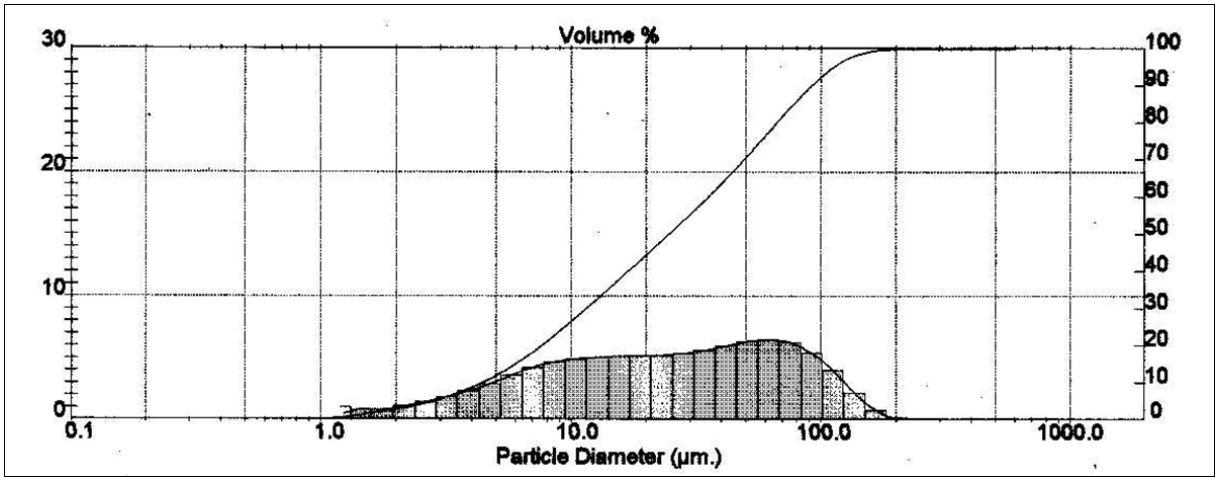

Figure 5. 11: Fly Ash Particle Size Distribution (Mastersizer,2003)

From the literature survey it was learned that the ESP efficiency is greatly affected by fly ash particle size. The particle size is a function of the migration velocity as stipulated in equation 2.1. Figure 5. 1 is a fly ash particle size distribution graph developed from the fly ash obtained from Lethabo Power Station. From the graph it is evident that the bulk of the particle sizes range between 8 µm and 30 µm which is the particle size range used for the simulations

6 CONCLUSION

As stated, the ESP simulation model was validated by the following Lethabo test data:

- **Simulation no. 1** was done based on the original Lethabo baseline figures for MCR, obtained from the C-Schedule design data (C-schedule, 1985)
- **Simulation no. 2** was based on the airflow optimisation tests at varying coal quality (Storm, 1998). The full load test at 627.5 MW where specification coal (mid-range quality) was burned and the optimum airflow was supplied for maximum thermal efficiency. These tests are named the revised baseline, since the PFFR guidelines for Lethabo were adapted, based on these tests.
- **Simulation no. 3** was done using the data of a complete ESP efficiency test executed in August 2011. (Inthuu measurements cc, 2011), as described in chapter 4. The U2 full load test with a dirty furnace (not sootblown prior to the test) data was used.

6.1 INTERPRETATION OF RESULTS

The first objective of this study is to develop an ESP simulation model and validate the calculated values with test data. Table 6. 1 depicts the correlation between 3 verification models and the test values.

Model verification no. 1 (table 6.1) is a simulation with the design baseline C-Schedule values. The input values for the combustion model and ESP simulation model are obtained from the original design data. Lethabo Power Station was designed for a particulate emission opacity value of 57 mg/Nm^3. The constants in the program for the effective migration velocity and the constant for the Deutsch equation were set to match the measured opacity. The Deutsch equation constant has a range of 0.5 – 1.0. This constant was set to 0.75 (mid-range) to enable flexibility. Thereafter the constant for the effective migration velocity was set with the Microsoft Excel “goal seek” function to produce a result matching the design value of 57 mg/Nm^3 for stack opacity.

Model verification no. 2 is a simulation with the data entered from the revised PFFR baseline test as mentioned above. This is the actual test data including the coal quality, coal flow, airflow supplied, airheater, furnace and ESP leakage, as well as the gas analysis measurements (O_2%, etc.). The effective migration velocity as well as the Deutsch equation constant remained unchanged for this simulation. The calculated stack opacity then differed with the measured test value by a small margin. The final customisation of the simulation model was then done by iterating

the ash particle size to a value to satisfy both simulations 1 and 2, the calculated values matching the measured stack opacity. This was possible when an ash particle size of 14 μm was used in both simulations 1 and 2. The opacity measured during the test used in simulation was 51 mg/Nm^3, while the simulation model calculated an opacity value of 50 mg/Nm^3. The simulation model still produced measured and calculated values of 57 mg/Nm^3 for stack opacity with the data of the C-Schedules (simulation 1) with the same values for the Deutsch equation and migration velocity constants as well as the same ash particle size (14 μm). These settings within the simulation model is satisfactory, since the mentioned constants are within the midrange allowed for each and the ash particle size of 14 μm is in the midrange of the normal distribution curve for Lethabo ash particle size. The normal distribution curve covers a range of 9 – 24 μm with significant percentages.

Model verification no.3 used data from the U2 ESP efficiency test conducted in August 2011 as mentioned above. The constants in the program for the effective migration velocity and the constant in the Deutsch equation remained unchanged, as in simulation 1 and 2. Although the particle size ranged from 19 - 26 μm between the four ESP casings, the opacity measured during this test was measured as 86 mg/Nm^3, while the ESP simulation model calculated an opacity value of 84 mg/Nm^3.

The performance of the simulation model can be considered satisfactory based on the degree of accuracy when comparing the calculated and measured values of simulations 1, 2, and 3. A Summary of these results can be seen in table 6.1. The results from the ESP simulation model correlate well with the test data for all three simulations. The ESP simulation model can thus be considered suitable and adequately reliable for ESP simulations.

The ESP simulation model which was developed for this study can therefore be used to:

- Identify deviations between the design base and the current state of the plant, and predict the effect thereof; in terms of stack opacity.
- Predict the particulate emissions when considering an ESP enhancement technology; and
- Evaluate the relative impact of specification dependent and independent parameters and their separate effect on ESP performance.

Table 6. 1: Summary of model verifications

no	TEST/SIMULATION Operating Conditions	ASH in coal [%] A/R	Fly-ash Burden [kg/s]	A/HTR Leakage [kg_{AIR}/s]	O_2 [% Volumetric Dry] Econ. Outlet	O_2 [% Volumetric Dry] A/HTR outlet	O_2 [% Volumetric Dry] ESP outlet	Gasflow ESP inlet [Am^3/s]	T_{GAS} ESP inlet [°C]	ESP Power Supply [kV]	ASH Fineness Distribution [µm]	ESP η [%]	Stack Opacity [mg/Sm^3]	Δ Opacity [mg/Nm^3]
1	Design Baseline C-Shedules 1985	31.3	28.5	66 (10.2%)	3.6	5.2	5.6	997.8	132	39	14	99.88	57	0
2	Revised Baseline and Tests 1997	42.2	41.7	36 (6.9%)	1.6	2.7	3.4	864.9	151	39	14	99.95	50	1
3	U2 Test 1 SO_3 Dirty Boiler 2011	39.0	43.3	50 (8.4%)	3.9	5.1	5.6	1117.1	158	37	21	99.76	84	2

Table 6.2 indicates a significant variation between the design base values and the current values obtained from the ESP efficiency test. The table also indicates the particulate emissions produced under each of the operating conditions. This highlights the need for quality maintenance and workmanship during maintenance opportunities. However, when keeping the entire plant and coal quality deterioration in mind, one must have an appreciation for the deterioration in the overall plant performance.

Table 6. 2: Comparison between design base and current operating conditions

Variable	Unit	Design base	Current operating condition
Volume flow	m^3/s	997	1117
Gas temperature	°C	135	160
Dust burden	g/m^3	32.5	33.4
% ash in coal	%	35	41
ESP power supply	kV	40	37
Uniform flow distribution		uniform	non-uniform
Particle treatment time	s	28	19.92
ESP gas velocity	m/s	1.2	1.75
Particulate emissions	mg/Nm^3	57	86

The second objective of this study is thus to utilise the model to predict demonstrate the greater impact on ESP performance when the ESP is operated with out-of-specification parameters.

Chapter 3.3, discusses whether an ESP enhancement technology could be considered when there is such a vast difference between the design base and the current operating conditions. The answer to the question of whether it could be justified to spend the capital expenditure on ESP enhancement technologies when the desired emission levels could be achieved by operating at the design base can now be evaluated. The problem of high particulate emission levels in Eskom can therefore be addressed by reinstating the ESP's to the design base and thereafter considering the installation of ESP enhancement technologies.

The third objective is to categorise the various parameters by identifying the magnitude of how much each parameter contribute to poor ESP performance. It must be noted that the original design base does not include SO_3 injection. SO_3 injection was only installed in 1998 at Lethabo (Bosch, 1998). In the following simulations all other variables were kept constant, except for the variable to be evaluated. Table 6.3 indicates the significance of a change in the following variables on ESP performance:

- Ash content in coal
- High fly ash burden
- Biased fly ash distribution
- High air heater leakage
- High gas volume flow
- Biased gas volume distribution
- High ESP inlet temperature
- Biased ESP inlet temperature
- ESP power supply
- Ash particle fineness

Simulation 1 and 2 (table 6.3): Effect of high ash content in coal with and without SO_3 injection:

The design base C-schedule model was used for this simulation, since the design coal quality had 30.7% ash content. All other parameters were kept constant except for the coal analysis. The simulation with which this was compared was a coal analysis of the airflow optimisation low grade coal test which had an ash content of 46.1%. In order to combust this lower specification coal, more air is required. The O_2% readings increased at the burner outlet, air heater outlet and the ESP outlet also increased due to the higher airflow supplied. The gas volume flow thus increased slightly from 997.8 Am^3/s to 1004.1 Am^3/s. The model predicted a particulate emission increase from 57 mg/Nm^3 to 99 mg/Nm^3 without SO_3 injection and the derived value to 56 mg/Nm^3 with SO_3 injection, due to high ash content in coal. These are actual test values used to produce a real case scenario for high ash content.

Simulation 3 and 4 (table 6.3): Effect of high air heater leakage and high airflow:

The revised baseline and test of 1997 was used to simulate the effect of high air heater leakage and high airflow. The air heater leakage was increased from 6.9% to 20%. The airflow was increased from 864.9 Am^3/s to 988.1 Am^3/s. The burner outlet O_2% reading remained the same but the air heater and ESP outlet O_2% readings changed from 2.7% to 5% and 3.4% to 5.5% respectively. The particulate emissions increased from 50 mg/Nm^3 to 109mg/Nm^3 without SO_3, and a calculated 61 mg/Nm^3 with SO_3. This simulation thus also predicts the effect of high gasflow.

Simulation 5 and 6 (table 6.3): **Effect of biased gas flow distribution between casings:**

The revised baseline and test of 1997 was used for this simulation. The total gas volume flow is artificially distributed as follows: LHO 15%, LHI 30% RHI 40% RHO 15%. This scenario forced some casings to pass high volume flows while other casings were deprived of the average gasflow. The outlet emissions for each casing were: LHO 2 mg/Nm^3, LHI 542 mg/Nm^3, RHI 2145 mg/Nm^3, RHO 2 mg/Nm^3. When considering equation 2.2 (Deutsch equation) it is understandable that the casing efficiency will be significantly affected by vast variations in volume flow. The simulation predicted the weighted average particulate emissions of the stack to 673 mg/Nm^3 without SO_3 injection and a calculated 210 mg/Nm^3 with SO_3 injection.

Simulation 7 and 8 (table 6.3): **Effect of high gas temperature:**

The design base C-schedule model was used for this simulation. It must be noted that the gas temperature has an influence on the volume flow (as a constant mass flow of gas expand, the volume flow will increase). In this simulation the higher temperatures' influence on only gas viscosity and ash resistivity is to be predicted. Thus, for this simulation the volume flow was artificially kept constant while only the gas viscosity and ash resistivity was varied with changes in temperature. The reason for this is that the volume flow can be increased by the draft group fans, and not only by temperature. The gas temperature was increased from 132 °C to 185 °C. Due to this temperature change the particulate emission increased from 57 mg/Nm^3 to 116 mg/Nm^3 without SO_3 injection and 56 mg/Nm^3 with SO_3 injection.

Simulation 9 and 10 (table 6.3): Effect of biased gas temperature between casings:

The design base C-schedule model was used for this simulation. The temperature distribution is as follows: LHO 130°C, LHI 145°C RHI 180°C RHO 160°C. For this simulation again only the influence on gas viscosity and ash resistivity is predicted by temperature. The particulate emission increased from 57 mg/Nm^3 to 76 mg/Nm^3 without SO_3 injection and 43 mg/Nm^3 with SO_3 injection.

Simulation 11 to 14 (table 6.3): Effect of varying power supply:

The revised baseline of the 1997 test was used for this simulation. The power supply was varied between 30 kV and 40 kV. This is the average high and low ranges of conventional transformer rectifiers. The migration velocity is a function of the electrical field strength (kV/cm), where the Deutsch equation is a function of the migration velocity. The particulate emissions of 50 mg/Nm^3 were reduced to 40 mg/Nm^3 without SO_3 and 23mg/Nm^3 with SO_3 when the average power supply is

raised to 40 kV. The particulate emissions increased to 277 mg/Nm^3 without SO_3 injection and 155 mg/Nm^3 with SO_3 injection for an average power supply of 30kV.

Simulation 15 to 18 (table 6.3): Effect of fly ash fineness:

The design base C-schedule model was used for this simulation. For this simulation the average particle size ranged from 10 µm to 18 µm. The migration velocity is a function of the ash particle size, where the Deutsch equation is a function of the migration velocity. The measured particulate emissions of 57 mg/Nm^3 is predicted to increase to 338 mg/Nm^3 without SO_3 injection and 217 mg/Nm^3 with SO_3 injection for an average ash particle size of 10µm. The measured particulate emissions of 57 mg/Nm^3 is predicted to decrease to 8 mg/Nm^3 without SO_3 injection and 5 mg/Nm^3 with SO_3 injection for an average ash particle size of 18 µm.

It is observable that some simulations have a high efficiency while still having high emissions. The fly ash burden measured in kg/s, for some simulations is significantly increased due to the ash percentage in coal and the flow distribution. It is for this reason that, for a higher fly ash burden, the efficiency remains the same while also seeing an increase in particulate emissions.

Table 6. 3: Summary on comparison of ESP Performance

SUMMARY ON COMPARISON OF ESP PERFORMANCE

Test no	TEST/SIMULATION Operating Conditions	ASH in coal [%] A/R	Fly-ash Burden [kg/s]	A/HTR Leakage [$kg_{A/HTR}$/s]	O_2 [% Volumetric Dry] Econ. Outlet	A/HTR outlet	ESP outlet	GASFLOW ESP inlet [Am^3/s]	T_{GAS} ESP inlet [°C]	ESP Power Supply [kV]	ASH Fineness Distribution [µm]	ESP η [%]	Stack Opacity [mg/Sm^3]	Δ Opacity [mg/Nm^3]
1	High Ash in Coal Simulation	46.1	47.8	66 (10.2%)	4.7	6.2	6.6	1004.1	132	39	14	99.98	99	-42
2	High Ash in Coal Simulation SO_3	46.1	47.8	66 (10.2%)	4.7	6.2	6.6	1004.1	132	39	14	99.97	56	1
3	High A/HTR Leak & Airflow Simulation	42.2	41.7	120 (20%)	1.6	5.0	5.5	988.1	151	39	14	99.86	109	-59
4	High A/HTR leak & Airflow Simulation SO_3	42.2	41.7	120 (20%)	1.6	5.0	5.5	988.1	151	39	14	99.92	61	-11
5	Biased Gasflow Simulation	42.2	41.7	120 (20%)	1.6	5.0	5.5	988.1	151	39	14	99.9	673	-623
6	Biased Gasflow Simulation SO_3	42.2	41.7	120 (20%)	1.6	5.0	5.5	988.1	151	39	14	99.94	210	-160
7	High Gas Temp. Simulation	31.3	28.5	66 (10.2%)	3.6	5.2	5.6	997.8	185	39	14	99.95	116	-59
8	High Gas Temp. Simulation SO_3	31.3	28.5	66 (10.2%)	3.6	5.2	5.6	997.8	185	39	14	99.97	56	1
9	Biased Gas Temp. Simulation	31.3	28.5	66 (10.2%)	3.6	5.2	5.6	997.8	132	39	14	99.96	76	-19
10	Biased Gas temp. Simulation SO_3	31.3	28.5	66 (10.2%)	3.6	5.2	5.6	997.8	132	39	14	99.98	43	14
11	Varying Power supply Simulation	42.2	41.7	36 (6.9%)	1.6	2.7	3.4	864.9	151	30	14	99.92	277	-227
12	Varying Power supply Simulation	42.2	41.7	36 (6.9%)	1.6	2.7	3.4	864.9	151	40	14	99.96	40	10
13	Varying Power supply Simulation SO_3	42.2	41.7	36 (6.9%)	1.6	2.7	3.4	864.9	151	30	14	99.94	155	-105
14	Varying Power supply Simulation SO_3	42.2	41.7	36 (6.9%)	1.6	2.7	3.4	864.9	151	40	14	99.96	23	27
15	Varying Ash fineness Simulation	31.3	28.5	66 (10.2%)	3.6	5.2	5.6	997.8	132	39	18	99.98	8	49
16	Varying Ash fineness Simulation	31.3	28.5	66 (10.2%)	3.6	5.2	5.6	997.8	132	39	10	99.89	338	-281
17	Varying Ash fineness Simulation SO_3	31.3	28.5	66 (10.2%)	3.6	5.2	5.6	997.8	132	39	18	99.99	5	52
18	Varying Ash fineness Simulation SO_3	31.3	28.5	66 (10.2%)	3.6	5.2	5.6	997.8	132	39	10	99.88	217	-160

Based on the content of Table 6.3, these various process conditions and parameters can be categorised as indicated in Table 6.4. From the seven simulations it can be concluded that biased gas flow distribution has the most significant negative impact on ESP performance.

Table 6. 4: Categorised process conditions and parameters that influence ESP performance.

	Out of the norm operating condition	Mitigation
1	Biased gas flow	• Ensure balanced draft group • Minimise air heater leakages both left hand and right hand • Ensure duct guide vanes are in as designed state
2	Fly ash particle size	• Ensure milling plant is performing according to specified standard
3	ESP power supply	• Optimisation of rapping philosophy • Optimisation of power supply
4	High gas temperatures	• Ensure air heater packs contribute to specified HX_{EFF} • More frequent sootblowing
5	High air heater leakages and high volume flow	• Ensure air heater performance is according to design specifications
6	Ash percentage in coal	• Ensure the contractual agreement with regards to coal quality is enforced. • Ensure specification grade coal is supplied
7	Biased gas temperature	• Ensure balanced air heater performance

When evaluating these seven factors, it can be concluded that the air heaters (primary and secondary) have a significant impact on four of the seven factors. This also demonstrated that the upstream independent variables have significant impact on ESP performance, and the ESP cannot be optimised or enhanced in isolation.

6.2 RECOMMENDATIONS

ESP system engineers and operators must have an appreciation of the consequences of not operating an ESP and furnace combustion according to design. ESP system engineers and operators should operate the entire power generation process holistically.

It is recommended that all Eskom plants equipped with ESPs must undertake an ESP efficiency test every three years. This will ensure the identification of deviations from the design base as well as determining the current status of the plant.

ESP enhancement technologies could be very effective in reducing particulate emissions on Eskom's ESP's, though this could only be achieved once the dependent and independent parameters are maintained and according to the design specifications.

The consequences of operating the furnace combustion parameters with the degraded state of the air heaters will eventually emanate in high emissions. It is therefore recommended that air heaters must always be maintained according to design specifications.

6.3 FURTHER STUDIES

- Existing CFD simulation programs, customised for Lethabo should be used to determine the gas distribution at the ESP inlet, as well as to determine how the flow develops through the ESP. One could determine the gas distribution at the inlet of each ESP field and compute the effect of various velocity profiles through the ESP, also see (Schmitz, Pretorious, & Gibson, 1998). This should also be applied to incorporate skew flow for improved opacity.
- The determination of the effect of current density on migration velocity as well as the effect of various discharge electrode designs, should be investigated.
- The development of a real time process monitoring system where the inputs for the combustion model and the ESP simulation model are extracted from a real time monitoring system.
- The installation of an online coal analyser can be invaluable.
- The determination of fly ash resistivity with variation of SO_3 gas injection rates can prove beneficial and cost saving.

7 REFERENCES

Arrondel, V., Bacchiega, G. & Gallimberti, I. 2001. Esp modelling for industrial application. Alabama: ICESP VIII.

Bäck, A. 2006. Enhancing ESP efficiency for high resistivity fly ash by reducing the flue gas temperature. 11th International Conference on Electrostatic Precipitation. Sidney: Alstom Power Sweden.

Bickelhaupt, R. 1979. A technique for predicting ash resistivity.Washington,DC: EPA.

Bosch, F. 1998. Investigation into suitability of SO_3 FCG for Lethabo. Johannesburg: Eskom.

Chambers, M. 2008. Improving ESP performance in a short time. Concord: WPCA.

Faulkner, M. & DuBard, J. 1984. A mathematical model of electrostatic precipitation. Chicago:EPA.

Gaikwad, R.P., Sloat, D.G., Altman, R. & Chang, R.L. 1993. Economic evaluation of electrostatic precipitators retrofit options. http://www.isesp.org/ICESP%20V%20PAPERS/PDFS/ICESP_V_09_06_1-18.pdf:. Date of access: 30 Sep. 2013.

Gooch, J., P. & Francis, N. 1979. A theoretical based model for the calculation of electrostatic pricipitator performance. Alabama: Southern Research Institute.

Harris, W. 2003. Electrostatic precipitator maintenance guide, Vol 1. California: EPRI.

Hein, A.G. & Gibson, D. 1993. Skewed gas flow technology improves precipitator performance eskom experience in South Africa. Johannesburg: ESKOM.

Herder, H. & Strydom, D. 2012. High frequency switch mode power supply for electrostatic precipitators. Johannesburg: NWL.

Paker, K.R. 1997. Applied electrostatic precipitators. London: Blackie Academic & Professional.

Kim, S., Park, H. & Lee, K. 2001. Theoretical model of electrostatic precipitator performance for collecting polydisperse particles. *Journal of electrostatics*, 50:177-190.

Kirsten, M. & Karlsson, A. 2006. Economical aspects of energising electrostatic precipitators with high-frequency switched power supplies.http://www.isesp.org/ICESP%20X%20PAPERS/PDFS/Paper%207A2.pdf. Date of access: 30 Sep. 2013.

Knapik, J. 2012. Process impacts on esp performance. Plainfield: WPCA

Kocik, M., Dekowski, J. & Mizeraczyk, J. 2005. Particle precipitation efficiency in an electrostatic precipitator. *Journal of electrostatics*, 63: 761–766

Lillieblad, l. & Maurizson, C. 2006. Upgrade technologies for electrostatic precipitators. http://www.isesp.org/ICESP%20X%20PAPERS/PDFS/Paper%208A2.pdf. Date of access: 30 Sep. 2013.

Jedrusik, A. S. 2006. Experimental and calculated values of migration velocity as a parameter of precipitation process in electrostatic precipitators . http://www.isesp.org/ICESP%20X%20PAPERS/PDFS/Paper%208B2.pdf. Date of access: 30 Sep. 2013.

McCain, J. D. 2007. Effects of temperature on esp performance. First Energy ESP Seminar . WPCA.

Mudry, R. 2002. ESP Gas flow fundamentals. ESP/FFP Round Table & Exposition. Airflow Sciences Corporation.

Munson, BR., Young D.F. & Okiishi T.H. 2006. Fundamentals of fluid mechanics. Hoboken, NJ: Wiley.

Noda, N., & Makino, H. 2010. Infuence of operating temperature on performance of electrostatic precipitator for pulverized coal combustion boiler. Advanced powder technology , 21: 495-499.

Nolan, P. 1996. Emission control technologies for coal-fired power plants. Beijing: Babcock & Wilcox.

Popvici, F. 1996. Esp and ffp basics. Johannesburg: Beier Albany.

Porle, K., Francis, S. l. & bradburn, K. M. 2005. Electrostatic precipitators for industrial applications. Brussels: Rehva.

Rasul, m. & Zhou, J 2006. The influence of flow distribution on the performance improvement of electrostatic precipitator. http://www.isesp.org/ICESP%20X%20PAPERS/PDFS/Paper%202A1.pdf. Date of access: 30 Sep. 2013.

Schmitz, W. Pretorious, L. & Gibson, D. 1998. Esp performance prediction and flow optimisation using CFD. http://www.isesp.org/ICESP%20X%20PAPERS/PDFS/Paper%202A1.pdf. Date of access: 30 Sep. 2013.

Steyn, F. Baidjurak, L. & Hansen, R. 2006. Fabric filter retrofits and electrostatic precipitator upgrade technology.http://www.isesp.org/ICESP%20X%20PAPERS/PDFS/Paper%209C1.pdf. Date of access: 30 Sep. 2013.

Storm, C.P. 1998. A macroscopic determination of the impact of Lethabo coal quality upon the optimum combustion air quantity. Potchefstroom: PU for CHE. (Thesis-PhD).

White, H.J. 1963. Industrial electrostatic precipitation. Reading, Mass: Addison-Wesley.

8 APPENDIX A

ESP operating philosophy

8.1 EPS COMPONENTS

An ESP consists of various components; each of these components contributes to the successful operation of a total particulate removal system. This section describes the basic function and location of the most common components found in ESP's.

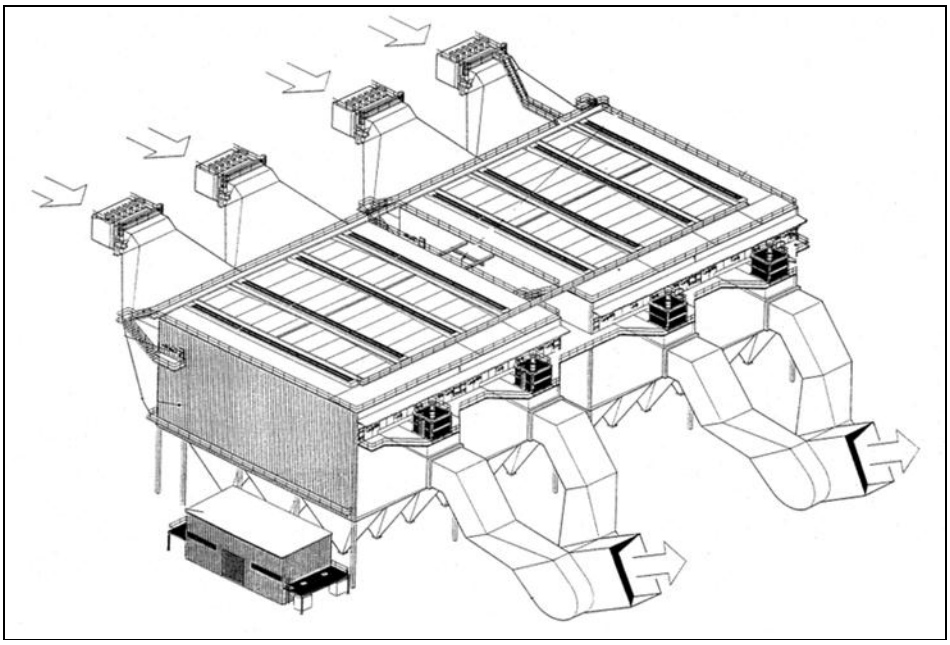

ESP with 4 parallel casings

The above figure represents a three-dimensional drawing of an ESP. From the picture it can be seen that this ESP has four parallel casings. The reference to each casing when looking in the direction of flow is: Left hand outer (LHO), Left hand inner (LHI), Right hand inner (RHI) and Right hand outer (RHO). When referring to the ESP efficiency or ESP performance it is the combined efficiency of the 4 casings, not one casing alone, unless specified otherwise.

8.1.1 STRUCTURAL

The components of an ESP are assembled in a gas-tight and weather-proof casing as indicated in the figure below.

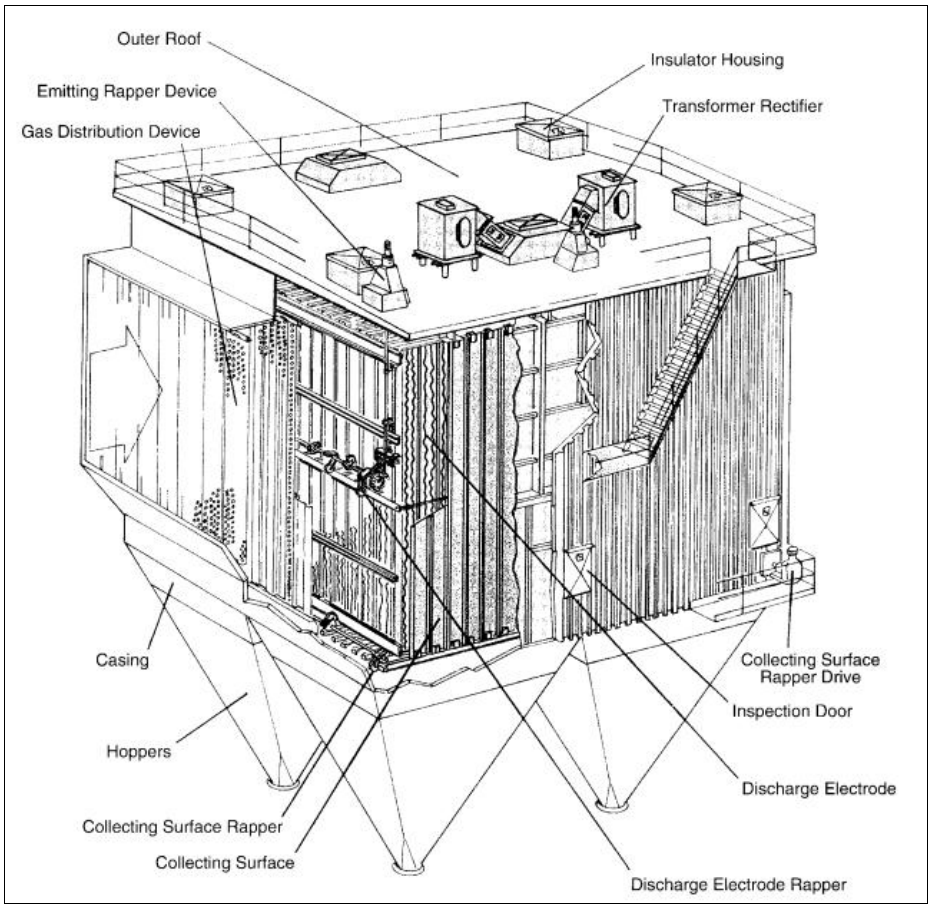

Figure 8. 1:ESP components (Popvici, 1996)

The important mechanical en electrical components are discussed in short:

8.1.2 MECHANICAL COMPONENTS

- **Discharge electrodes**

The purpose of the discharge electrodes (DE) is to provide a source of ionisation to charge and provide an electrostatic field to drive the particles to the collecting electrodes. There are many different discharge electrode designs as indicated in the figure below. Different materials to be collected have different collection rates with various discharge electrode designs. The design considerations for discharge electrodes are: performance, cost, ease of installation, ease of alignment, sensitivity to misalignment, rap-ability and reliability.

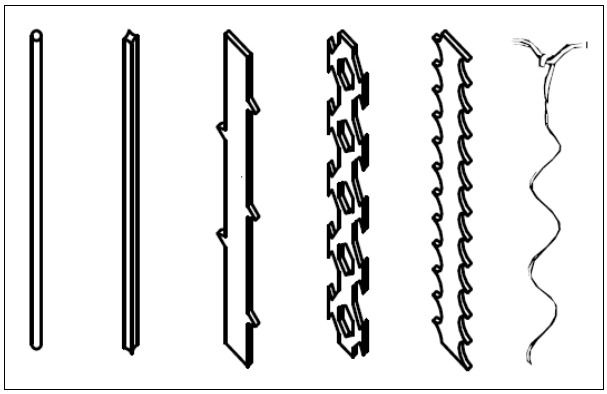

Figure 8. 2: Different discharge electrode designs

The type of the electrode is largely dependent on the gas constituents and dust properties. The ionic wind flowing from the discharge electrode to the collector electrode is largely dependent on the discharge electrode design.

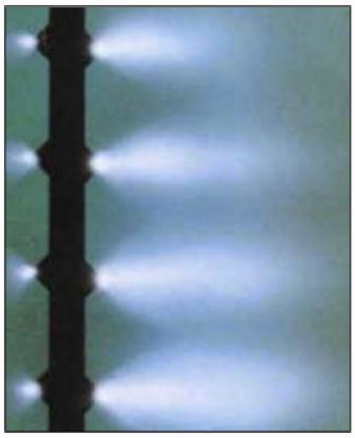

Figure 8. 3: Corona from sharp spikes produces high intensity ionisation.

The figure above indicates the corona formed on the spikes of the electrode.

- **Collecting electrodes**

The purpose of the earthed collecting electrode (CE) is to collect the ionised particles and temporarily keep them attached to the collector plate until rapped. The design considerations for the CE are: performance, cost, ease of installation, ability and ease of alignment, rap-ability, reliability and re-entrainment minimisation. Some ESP manufacturers prefer different profiles and designs, some are designed for strength and rigidity and other for better collection efficiency. The preference of CE profile is largely dependent on the manufacturer's philosophy and experience.

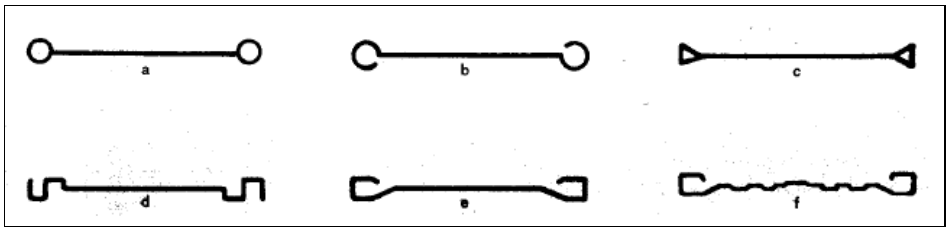

Figure 8. 4:Different collector electrode designs

- **Rapping systems**

The two figures below indicate the rapping systems of the CE and DE respectively. The tumbling hammer design is the most common for CE and DE rapping system in Eskom. A series of hammers are connected to the shaft that rotates slowly. It is powered by a motor situated on the outside of the ESP. In the case of the CE the rapper motors are installed on the side of the ESP next to the inspection doors. For the DE the rapper motor is installed in the ESP roof and by means of a crown wheel and pinion rack where the vertical rotation is transferred into horizontal rotation. As the shaft rotates the hammer impacts on an anvil connected to the DE or CE. The energy of the impact is transferred to the collector plates to dislodge the ash.

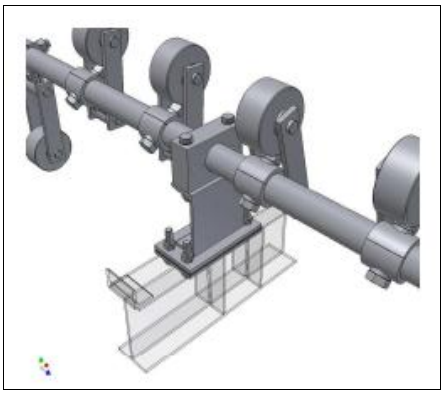

Figure 8. 5: Collector electrode tumbling hammer rapping system

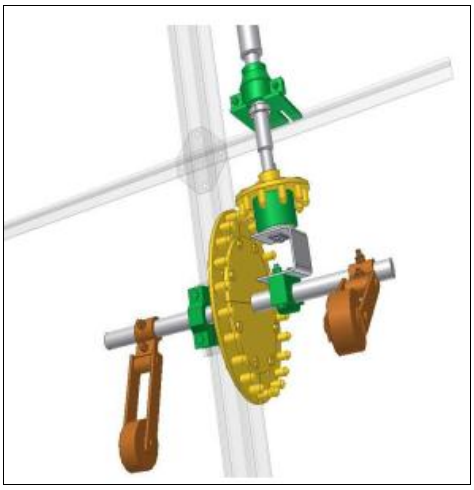

Figure 8. 6: Discharge electrode tumbling hammer system

- **Insulators**

The four blue cone-shaped components in the figure below are known as the support insulators. These insulators are manufactured from a non-conductive material like ceramic. The DE fields are energised via the centre of these non-conductive support insulators. The purpose of the insulators is to isolate the DE from the earthed components. If an earthed component comes into contact with a live component, the transformer supplying the field would short and trip. It is visible from the figure below that the entire DE field is hanging freely with the four ceramic insulator pots supporting the DE field.

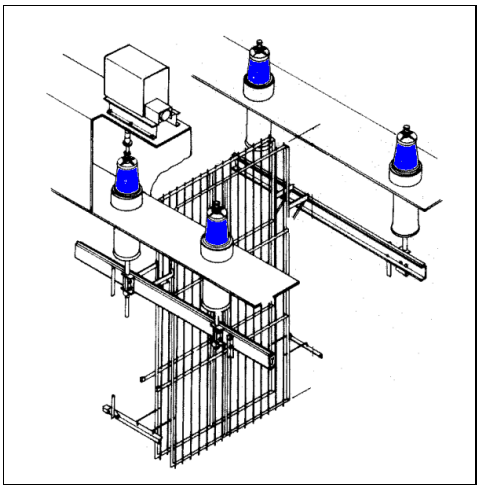

Figure 8. 7:Ceramic support insulators

- **Hoppers**

The hoppers are placed directly underneath each field. The hoppers are a temporary storage compartment to store the ash collected by the ESP fields. The ash is removed by means of the dust handling plant from where it is stored in ash bunkers. It is vital that the ash level in the hoppers never reach a level where the ash penetrates into the electrodes. Most hoppers are equipped with hopper level monitors to prevent overfilling of the hoppers. The damage caused by such an occurrence can equate to millions of dollars in damage to the plant. Firstly, the upward force of the ash damages the electrodes as the upward force compresses the electrodes to the ESP roof, causing the electrodes to buckle. Secondly, the hoppers are designed to store hundreds of tons of ash, but numerous incidents have been recorded where the ESP structure and hoppers are badly damaged due to overfull hoppers. It is therefore very important to operate the ESP with close to empty hoppers and to always ensure that the hopper level monitoring equipment is tested on a monthly basis.

8.1.3 ELECTRICAL COMPONENTS

- **Rapper controls**

Referring to chapter 2.12, the rapping of the electrodes are done at specific intervals for specific durations, these intervals and durations are controlled by controllers situated in the ESP substation. These settings can be controlled via the Plant Management System from the control room.

- **Hopper heaters**

The hoppers are equipped with a mesh-like heater element in the lower section of the hopper, ± 2.5 meters from the knife gate at the hopper exit. The purpose of these heaters is to keep the ash at a high temperature where the ash is fluent. Ash flows in much the same way as water at high temperatures; encouraging the de-dusting from the hopper to the dust handing plant. If the of ash cools down inside a hopper, de-dusting is very difficult as the ash tends to block the hopper exit shoot. On occasions like these, the plant has to be shut down and the ash must be removed manually.

- **Insulator heaters**

As mentioned earlier, the support insulators are manufactured using ceramic. One of the properties of ceramic is that it cannot withstand any thermal shocks. The insulators are equipped with heater elements to ensure the support insulators are always at a high temperature to eliminate the effect of thermal shocks.

- **Electrical power supply**

The ESP fields are powered by means of rectifier transformers which are situated on the ESP roof. The rating of these transformers varies in terms of milliamps and kilo volt output. The rating of the transformers supplying large ESP fields is in the range of 70 kV to 1500 mA. If a transformer supplies insufficient kV and mA to the ESP fields, the corona density will be insufficient which will result in poor particle charging and poor ESP efficiency. The latest High Frequency technology for power supply is discussed in chapter 3.2.4.

- **Voltage controllers**

The power supplied to the ESP's via the transformers is controlled by highly sophisticated controllers. In the case of older generation rectifier transformers, these controllers are situated in the ESP sub-station. The new generation High Frequency transformers are integrated units, where the transformer and the controller are both situated in the same housing. One of the capabilities of these controllers is that they were designed to learn the sensitivity of the sparking in the ESP. The controller will then charge the field to a maximum kV to just below the sparking point. This practice ensures that the maximum allowable kV is supplied to the ESP field which improves ionisation. The ramp and step functions are also controlled via the voltage controller.